Acta Pharmaceutica Sinica B 2026;16(5):3157−3174

Chinese Pharmaceutical Association
Institute of Materia Medica, Chinese Academy of Medical Sciences

Acta Pharmaceutica Sinica B

www.elsevier.com/locate/apsb
www.sciencedirect.com

ORIGINAL ARTICLE

A novel entry inhibitor targeting the stalk domain of the hemagglutinin of H1N1

Ying Gong[a,b,c,†], Tongyu Bi[b,d,†], Fuling Xiao[a,b], Dandan Xu[e], Xun Zhang[f], Han Wang[b,d], Peng Yu[g], Xiaoqian Yang[a], Jianping Zuo[a,b], Li Yang[a,b,h,*], Weibo Yang[b,d,*], Xiankun Tong[a,b,*]

[a]*Laboratory of Immunopharmacology, State Key Laboratory of Drug Research, Shanghai Institute of Materia Medica, Chinese Academy of Sciences, Shanghai 201203, China*
[b]*University of Chinese Academy of Sciences, Beijing 100049, China*
[c]*Northern Jiangsu People's Hospital, Yangzhou 225001, China*
[d]*State Key Laboratory of Drug Research, Shanghai Institute of Materia Medica, Chinese Academy of Sciences, Shanghai 201203, China*
[e]*Jiangsu Key Laboratory of Marine Pharmaceutical Compound Screening, College of Pharmacy, Jiangsu Ocean University, Lianyungang 222005, China*
[f]*School of Chinese Materia Medica, Nanjing University of Chinese Medicine, Nanjing 210023, China*
[g]*Department of Pathology and Institute of Molecular Pathology, The First Affiliated Hospital, Jiangxi Medical College, Nanchang University, Nanchang 330006, China*
[h]*Key Laboratory of Medical Molecular Virology (MOE/NHC/CAMS), Shanghai Frontiers Science Center of Pathogenic Microorganisms and Infection, School of Basic Medical Sciences, Shanghai Medical College, Fudan University, Shanghai 200000, China*

Received 18 March 2025; received in revised form 29 October 2025; accepted 3 December 2025

KEY WORDS

Influenza virus;
Entry;
Hemagglutinin;
Stalk domain;
F subdomain;
Membrane fusion;
Macrocyclic compound;

Abstract Influenza is a global health issue. Vaccines can protect humans from infection from influenza virus. When no suitable vaccine is available, anti-influenza drugs are the first treatment choice. Emergence of drug resistance necessitates development of novel anti-influenza virus drugs. We investigated a novel macrocyclic compound H1N1-17 using *in vitro* assays. Through evaluation of its antiviral effect against H1N1 and H3N2 viruses, compound H1N1-17 showed selective inhibition of H1N1 virus strains. Invasion of pseudo-H1N1 was blocked by H1N1-17 in the entry inhibition assay. Membrane fusion of H1N1 and the endosome mediated by the stalk domain of hemagglutinin was inhibited by H1N1-17. In the induction of a drug-resistant mutations assay, the resistant sites of H1N1 to H1N1-17 were located

*Corresponding authors.
E-mail addresses: yangli@simm.ac.cn (Li Yang), yweibo@simm.ac.cn (Weibo Yang), xktong@simm.ac.cn (Xiankun Tong).
[†]These authors made equal contributions to this work.

Peer review under the responsibility of Chinese Pharmaceutical Association and Institute of Materia Medica, Chinese Academy of Medical Sciences.

https://doi.org/10.1016/j.apsb.2026.02.003

Combination therapy

in the F subdomain of hemagglutinin, which is crucial for membrane fusion. Intraperitoneal administration of compound H1N1-17 protected mice challenged with lethal H1N1 from death and weight loss, and effectively alleviated lung injury caused by viral infection. Additionally, compound H1N1-17 exhibited synergistic anti-influenza activity with oseltamivir acid, which was of significance for combination therapy.

1. Introduction

Influenza, a periodic respiratory disease in humans caused by highly contagious viral infection, significantly affects human health. Influenza virus is mainly transmitted through aerosol droplets and usually causes moderate respiratory diseases. However, lower respiratory tract infections can lead to pneumonia and develop into acute respiratory distress syndrome, leading to death through respiratory failure. The World Health Organization estimates that annual influenza epidemics affect approximately 5%−20% of the world's population, resulting in around 3−5 million cases of severe illness and 300,000−500,000 deaths[1]. The main strains of influenza A virus that cause seasonal influenza in humans are H1N1 and H3N2. Seasonal influenza vaccination is the best way to prevent infection, but current vaccines offer limited protection because of rapid antigenic shift and drift in the virus[2].

Three types of drugs have been approved by the US Food and Drug Administration (FDA) to treat acute influenza: matrix protein 2 (M2) ion channel inhibitors, neuraminidase (NA) inhibitors, and polymerase complex inhibitors. Amantadine and rimantadine are adamantane drugs that can inhibit the activity of M2 ion channels[3], blocking entry of protons into the virus, inhibiting conformational changes of hemagglutinin (HA) induced by low pH, inhibiting membrane fusion of the virus and endosome[4,5]. Zanamivir, oseltamivir, and peramivir are NA inhibitors[6-8] that can inhibit the sialidase activity of NA and hinder release of viral particles from the surface of host cells[9]. The latest anti-influenza drug approved by the FDA is Baloxavir marboxil (BXM)—a novel influenza virus RNA polymerase inhibitor that inhibits activity of enzymes by binding to catalytic metal ions at the active site of the polymerase to inhibit virus proliferation[10,11]. Because most influenza virus have developed resistance to M2 ion channel inhibitors, these inhibitors are no longer recommended as clinical drugs. Currently, the first-line clinical treatments for influenza infection are zanamivir, oseltamivir, and peramivir. Several influenza virus strains have also developed resistance to NA inhibitors—a dilemma resolved by BXM. However, the rapid mutation of influenza viruses requires new anti-influenza drugs with novel mechanisms and new targets to combat their persistent threat.

Because HA plays an important role in the adsorption and membrane fusion stages of viruses[12], it is a good target to design treatment strategies for influenza virus infection[13,14]. With the development of various HA crystal structures, the structure and function of HA is better understood[15-17]. The HA protein is translated as an uncleaved HA0 precursor that cannot cause virus and endosome membrane fusion. During virus maturation, HA0 is further cleaved into an HA1/HA2 complex that can fuse in a low pH environment[18], folds into a trimer and then is glycosylated and acylated.

HA can be divided into receptor binding (R), esterase (E), membrane fusion (F), and membrane-anchored (M) subdomains[19]. HA is anchored to the viral envelope through the M subdomain. The head structure of HA comprises the sequence of HA1, with R and E subdomains forming a shallow depression in the head. The R subdomain is responsible for receptor binding, and the E subdomain plays a role in connecting R and F subdomains. The F subdomain is the main component of the stalk of HA, comprising HA2 and a portion of HA1. Helices A and B formed by the sequence of HA2 are the main components of the F subdomain. There is also a thermosensitive fusion peptide that is 23 amino acids long at the amino end of HA2. Many small molecules have been identified to target the stalk domain, the most conservative region in HA, to block virus infectivity by inhibiting membrane fusion mediated by HA[20-22].

Because of their high affinity and selectivity, macrocycles are being increasingly applied in drug discovery. Infectious diseases are the main therapeutic indications of macrocyclic drugs, and account for 44.4% of them. Recently, 80%−90% of macrocyclic and clinical candidate drugs have been derived from natural products. We previously constructed pseudo-natural macrocycles using an efficient modular biomimetic assembly strategy, and identified a compound with an EC_{50} of 2.30 μmol/L against H1N1 (A/Puerto Rico/8/34) as a macrocyclic oxime inhibitor of influenza H1N1[23]. A subsequent structure−activity research and drug-like optimization resulted in the discovery of the lead candidate H1N1-17, with potent antiviral activity (EC_{50} = 0.37 ± 0.12 μmol/L) and low cytotoxicity (CC_{50} = 129.5 ± 13.9 μmol/L). Herein, we demonstrate that compounds H1N1-17 blocks membrane fusion of H1N1 by interacting with the stalk domain of HA, and the potential interaction sites are located in the F subdomain of HA. We report intraperitoneal administration of compound H1N1-17 to protect H1N1-infected mice from death and weight loss—activity comparable with oseltamivir phosphate *in vivo*. We then demonstrate the synergistic effect of compound H1N1-17 and oseltamivir acid against H1N1.

2. Results

2.1. General method for chemistry

The commercial reagents and solvents were utilized without further purification in chemical synthesis. All reactions, unless otherwise stated, were performed under an argon atmosphere, and monitored by thin layer chromatography (TLC) with

0.15−0.2 mm precoated silica gel plates visualizing by irradiation with UV light (λ = 254 nm) or the developing agent ethanolic phosphomolybdic acid and heating. Flash chromatography was performed using silica gel (300−400 mesh). ^{1}H NMR and ^{13}C NMR spectra were generated in $CDCl_3$, CD_3OD, or DMSO-d_6 on Bruker Avance DRX spectrometers at 600/500/400 and 126/101 MHz. Low-resolution mass (ESI) data were collected using an Agilent 6110 Quadrupole LC/MS spectrometer. High-resolution mass (ESI) data were collected using an Agilent 6545 QTOFLC-MS spectrometer. The purity of the final compound was assessed *via* HPLC analysis utilizing the Shimadzu LC20ADXR high-performance liquid chromatography coupled with a diode array detector (DAD) and was confirmed to be >95%. HPLC condition included a Poroshell 120 column (EC-C18, 4.6 mm × 250 mm, 2.7 μm) with a flow rate of 1.0 mL/min. The eluent was 10%−40% CH_3CN in pure water (0−2 min), 40%−90% CH_3CN in pure water (2−20 min), and 90% CH_3CN in pure water (20−30 min). Compound H1N1-17 was synthesized *via* methods below (Scheme 1).

2.2. *Anti-influenza activity of H1N1-17 in vitro*

To determine the anti-influenza activity of H1N1-17, the replication of influenza A viruses (H1N1 or H3N2) was evaluated in Madin−Darby canine kidney (MDCK) cells 72 h after infection by RT-qPCR assays. The EC_{50} of H1N1-17 on H1N1 (A/Puerto Rico/8/34) replication was 0.37 ± 0.12 μmol/L, but the efficacy on H3N2 (A/Hong Kong/8/68) virus was relatively limited (Fig. 1A). Activities of H1N1-17 against other influenza A strains *in vitro* were also evaluated (Fig. 1B). H1N1-17 had similar activities against four H1N1 strains (A/Puerto Rico/8/34, A/California/07/2009 pdm09, A/WS/33, A/FM/1/47) but no apparent inhibitory effect on the replication of two H3N2 strains (A/Hong Kong/8/68, A/California/2/2014) and influenza B (B/Taiwan/2/62).

Anti-influenza activity was also detected by Western blot, and cytopathic effects (CPE) and immunofluorescence assays. Compound H1N1-17 significantly inhibited levels of H1N1 proteins, but had minor effects on viral proteins of H3N2 (Fig. 1C and D). H1N1-17 also alleviated CPE of H1N1 but not H3N2 infection in MDCK cells (Fig. 1E). Similarly, H1N1-17 significantly decreased the nucleoprotein of H1N1 but not H3N2 in MDCK cells (Supporting Information Fig. S1). Results of these methods were consistent, indicating that H1N1-17 specifically inhibit H1N1. H1N1-17 also inhibited the expression of H1N1 viral proteins in Calu3 (human-derived lung adenocarcinoma) cells (Supporting Information Fig. S2A and S2B). H1N1-17 also significantly alleviated CPE of H1N1 infection in Calu3 cells (Fig. S2C) and decreased the nucleoprotein of H1N1 (Fig. S2D), eliminating the impact of host factor on the anti-influenza activity of H1N1-17.

2.3. *H1N1-17 inhibits an early step of H1N1 virus infection*

To investigate how H1N1-17 acts, a time-of-addition assay was performed to determine at what stage of the virus infection it acted

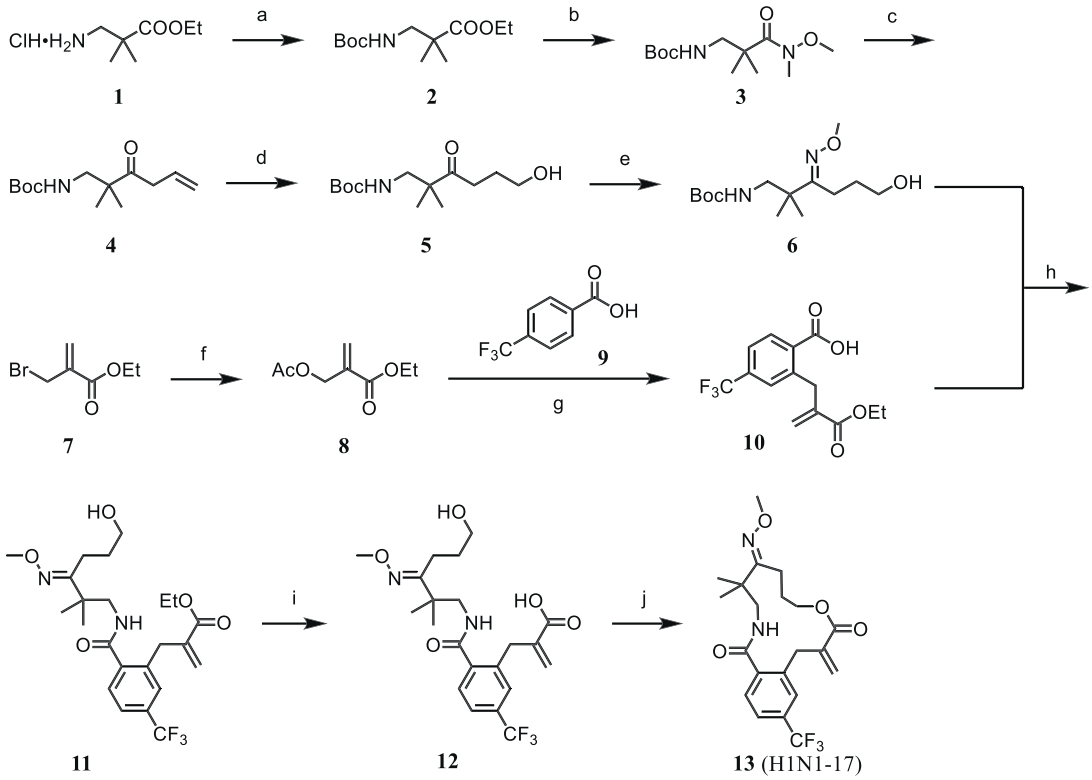

Scheme 1 Synthesis of compound H1N1-17. Reagents and conditions: (a) $NaHCO_3$, $(Boc)_2O$, acetone/H_2O = 1:1, 0 °C to rt; (b) *N*,*O*-dimethylhydroxylamine hydrochloride, ^{i}PrMgCl, THF, 0 °C to rt; (c) allylmagnesium chloride, THF, −60 °C; (d) (i) 9-BBN, THF, 0 °C to rt; (ii) H_2O, $NaBO_3 \cdot 4H_2O$, THF, 0 °C to rt; (e) methoxyammonium chloride, pyridine, 80 °C; (f) NaOAc, MeOH, 40 °C; (g) K_2CO_3, [Ru(*p*-cymene)Cl_2]$_2$, 2,2,2-trifluoroethan-1-ol, 65 °C; (h) (i) TFA, DCM, rt; (ii) HATU, DIPEA, DMF, 0 °C to rt; (i) NaOH, MeOH/H_2O = 1:1, 0−50 °C; (j) (i) 2,4,6-trichlorobenzoyl chloride, Et_3N, THF, 0 °C to rt; (ii) DMAP, THF, 40 °C.

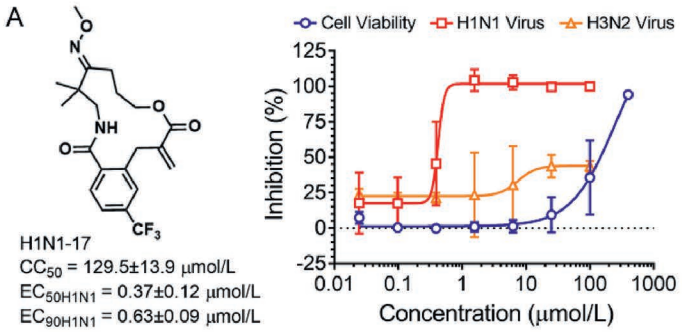

B

Influenza Virus Strains		EC_{50} (μmol/L)
Flu A (H1N1)	A/PR/8/34	0.37 ± 0.12
	A/California/07/2009 pdm09	0.87 ± 0.09
	A/WS/33	0.12 ± 0.05
	A/FM/1/47	0.29 ± 0.15
Flu A (H3N2)	A/Hong Kong/8/68	>100
	A/California/2/2014	>100
Flu B	B/Taiwan/2/6	>100

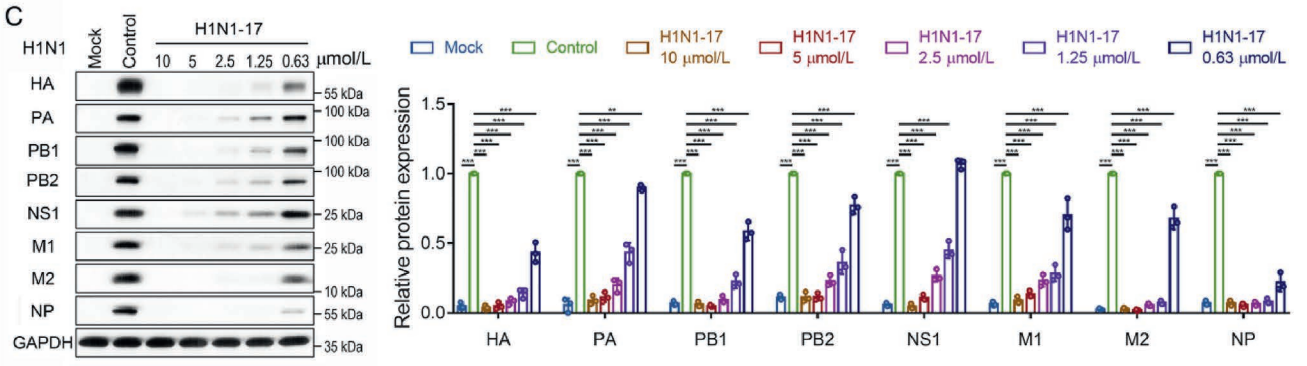

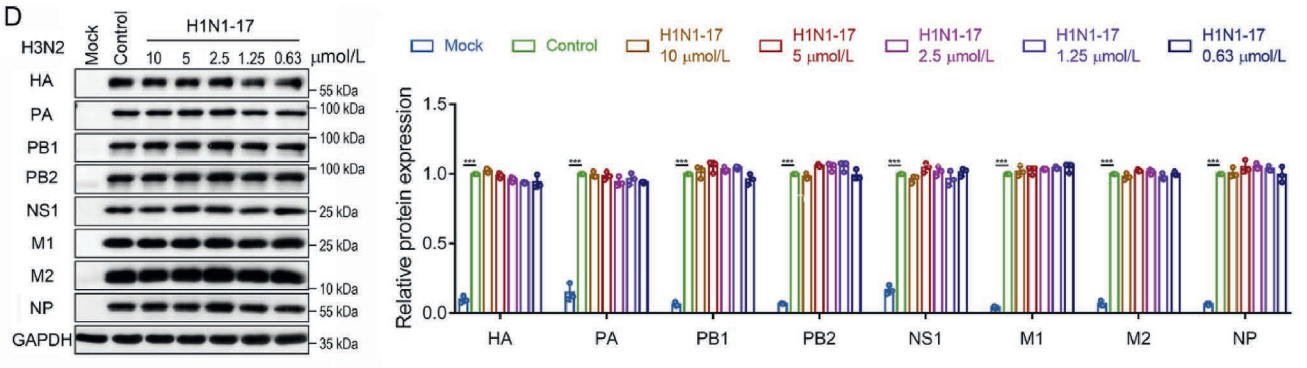

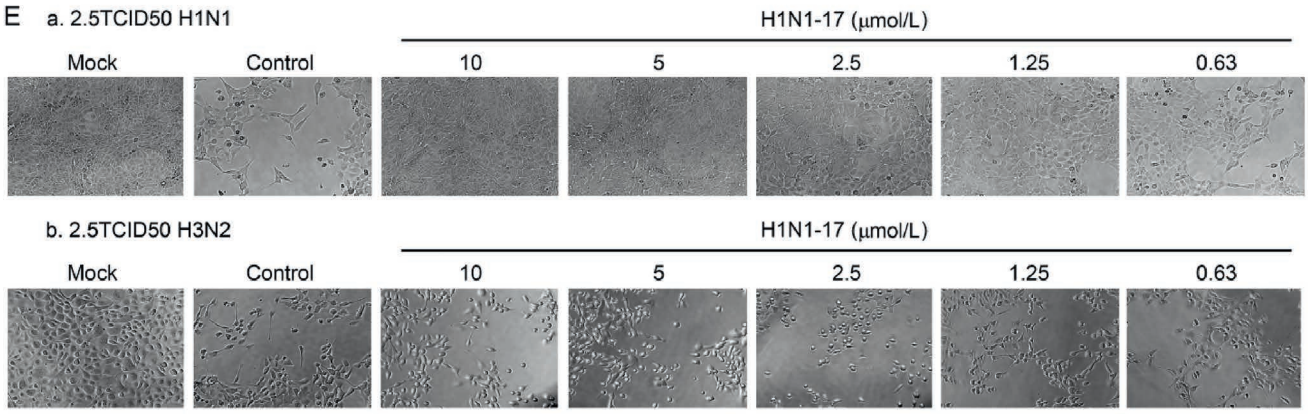

Figure 1 Effects of compound H1N1-17 on cell viability and multiplication of H1N1 (A/PR/8/34) and H3N2 (A/Hong Kong/8/68). (A) Chemical structure of compound H1N1-17 and its cytotoxicity and antiviral effects in MDCK cells. CC_{50}, 50% cytotoxic concentration; EC_{50}, 50% maximal effective concentration; EC_{90}, 90% maximal effective concentration. Values are means ± SD (n = 3). (B) EC_{50} values for compound H1N1-17 against indicated influenza virus strains *in vitro*. Values are means ± SD (n = 3). (C) Viral proteins of H1N1 in MDCK cells treated with compound H1N1-17 decreased in a dose-dependent manner in a Western blot assay. Relative quantification was shown on the right

(to determine when H1N1-17 had its maximal effect). Because it takes 8−10 h for influenza A virus to produce progeny viruses after virus attachment, six time-points (−2, 0, 2, 4, 8, and 24 h) for dosing were used, covering the life cycle of H1N1 virus strain (from attachment to progeny production). Following treatment, all viral RNAs from cell culture supernatants were detected 48 h post infection.

Apparent inhibition of virus amplification occurred when H1N1-17 was added at an interval from −2 to 2 h post virus infection. This time frame corresponds to early stages of influenza virus replication (*e.g.*, attachment, endocytosis, or membrane fusion). When the compound was added 8−24 h post infection, antiviral activity declined sharply (Fig. 2). These data suggested that H1N1-17 targets the early stage of H1N1 infection.

2.4. H1N1-17 blocks H1N1 membrane fusion mediated by the stalk domain of H1N1 HA

Viral attachment, endocytosis, and membrane fusion constitute the early stages of H1N1 infection, during which the membrane proteins HA and NA exert important activity[24]. These stages represent the entry of the virus into the host cell. We constructed a system of pseudo-type H1N1, H1N2 or H5N1 invading 293T cells to imitate the entry of H1N1, H1N2 or H5N1 into host cells, during which pseudo-type virus invasion was evaluated through quantitative detection of luciferase levels. H1N1-17 had selective activity against the infection of pseudo-H1N1 (EC_{50} = 1.04 ± 0.61 μmol/L) and pseudo-H1N2 (EC_{50} = 1.01 ± 0.21 μmol/L). However, H1N1-17 had little interference in the invasion of pseudo-H5N1 (Fig. 3A). Because two H1N1 membrane proteins (HA and NA) were involved in the invasion of pseudo-H1N1, HA and/or NA might be the target of H1N1. However, because the NA of H1N1 and H5N1 are identical, and the compound H1N1-17 had no activity against pseudo-H5N1, the probability of NA being a target for compound H1N1-17 is extremely low. We then explored whether H1N1-17 inhibited NA activity using a NA inhibition assay, and the result showed that H1N1-17 scarcely inhibited NAs of H1N1 and H3N2, indicating that H1N1-17 was not a NA inhibitor (Supporting Information Fig. S3).

Spontaneously, the HA became the key target because of its important role in viral attachment and membrane fusion. Entry of influenza viruses into host cells is initiated by attachment to sialic acid receptors, followed by important conformational changes of HA, and fusion with endosome membranes. Receptor-binding sites in the head of HA can bind to terminal sialic acids of glycoproteins and glycolipids under neutral pH conditions, causing virus adhesion and red blood cell agglutination[14]. A standard hemagglutination inhibition assay revealed that H1N1-17, liked anti-influenza drugs that did not target head domain of HA (pimodivir, favipiravir, zanamivir), did not inhibit hemagglutination of guinea pig erythrocytes caused by H1N1 viruses at 4 HAU (hemagglutination units) (Fig. 3B), suggesting that H1N1-17 did not affect receptor recognition or virus attachment. To explore the target of H1N1-17 after the attachment phase, H1N1 viruses were incubated with Calu3 cells at 4 °C for 1 h for adsorption without

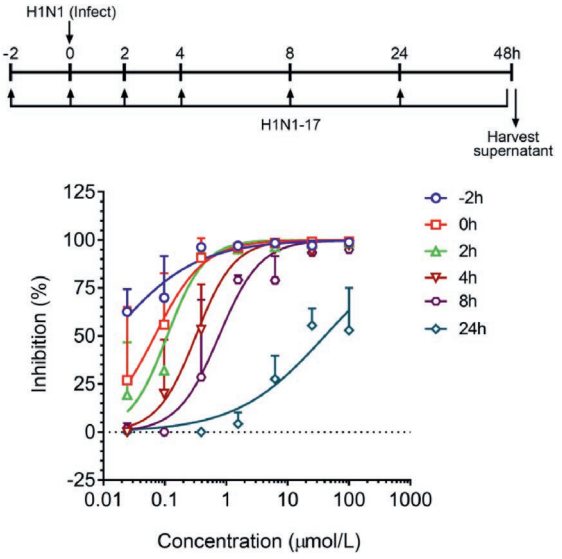

Figure 2 Compound H1N1-17 acted on the early stage of H1N1 infection. Time course of the addition of compound H1N1-17. Compound H1N1-17 was pre-incubated with Calu3 cells (−2 h, pre-infected), or added to H1N1-infected Calu3 cells at 0 (post-infected), 2, 4, 8, and 24 h. At 48 h after infection, viruses from the cell supernatant were harvested and quantified by one-step real time PCR assay. Antiviral activity of compound H1N1-17 gradually decreased with time. Values are means ± SD (n = 3).

endocytosis. H1N1-17 at serial dilutions was added at endocytosis (0 h post adsorption),membrane fusion (2 h), uncoating (4 h), and replication stages (8 h). After a single-round life cycle of H1N1 in cells, intracellular viral RNAs were extracted and determined. H1N1-17 significantly inhibited endocytosis and membrane fusion at 0 h post adsorption, and its antiviral activity gradually decreased with time and was almost gone 4 h post adsorption (Fig. 3C). HA protein undergoes conformational changes at low pH to drive membrane fusion. Conformational rearrangements of HA exposes trypsin receptors that can be digested by trypsin, and also exposes hydrophobic fragments that can cause hemolysis[25]. A standard hemolysis inhibition assay revealed H1N1-17 significantly inhibited hemolysis of guinea pig erythrocytes mediated by H1N1 virus in acidic conditions (Fig. 3D), demonstrating that H1N1-17 interfered with HA stalk-mediated membrane fusion.

2.5. H1N1-17 directly interacts with the HA protein of H1N1

To explore the interaction between the compound H1N1-17 and HA protein, a protein competition inhibition assay was designed. H1N1 viruses were incubated with Calu3 cells at 4 °C for 1 h for adsorption. Compound H1N1-17 or the mixture of H1N1-17 and three HA subtypes (H1, H3, H8) was added when the temperature rose to 37 °C to initiate endocytosis. After a 3-days treatment, cell viability and morphology were examined and viral RNAs from cell culture supernatants were determined to assess whether H1N1-17 antiviral activity was antagonized by HA protein.

(n = 3). Values are means ± SD. (D) Viral proteins of H3N2 in MDCK cells were invariable following treatment with compound H1N1-17 in a Western blot assay. Relative quantification was shown on the right (n = 3). Values are means ± SD. (E) Compound H1N1-17 alleviated the cytopathic effects of H1N1 but not H3N2 infection in MDCK cells. TCID50, 50% tissue culture infectious dose. Cell viability and morphology were examined microscopically using a 10 × objective (scale bar: 100 μm). *P < 0.05, **P < 0.01, and ***P < 0.001, by two-way Anova (or mixed model) in (C) and (D).

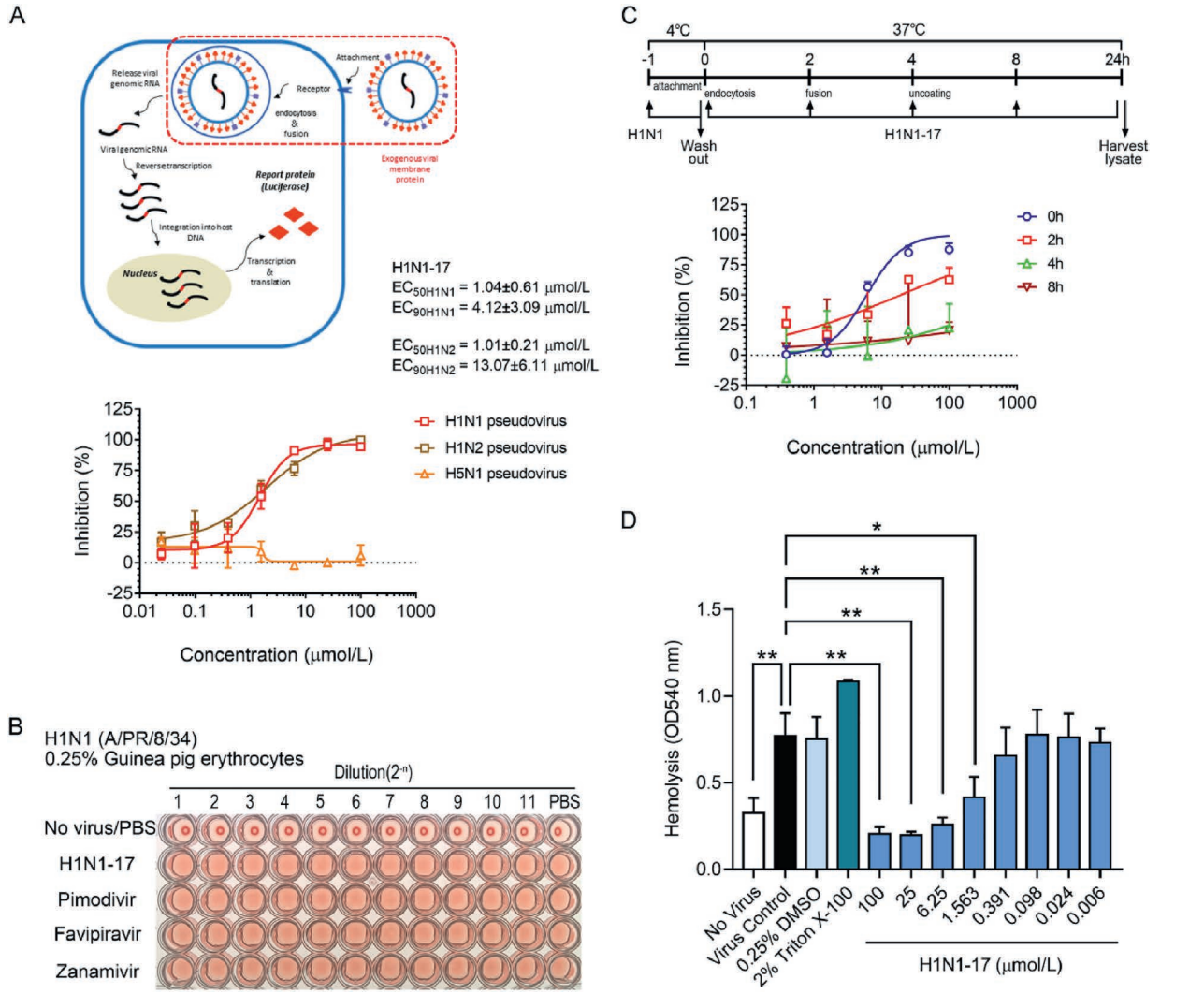

Figure 3 Mechanism of action of compound H1N1-17. (A) Pseudo-type H1N1, H1N2 or H5N1 models. The membrane protein (GP120/41) on the HIV-1 genome (black) was replaced with luciferase (claret), and the viral proteins Vpr (viral protein regulatory) and Nef (negative factor) were removed, and then modified with exogenous HA (H1 or H5, red) and NA (N1 or N2, lavender). Expression of luciferase on the HIV-1 genome was driven by entry of pseudo-type H1N1, H1N2 or H5N1. Compound H1N1-17 inhibited entry of pseudo-H1N1 and pseudo-H1N2 in a dose-dependent manner, but did not affect pseudo-H5N1 entry. Amounts of pseudo-type viruses entering cells are indicated by luciferase levels. Values are means ± SD ($n = 3$). (B) Compound H1N1-17 did not inhibit hemagglutination of guinea pig erythrocytes caused by H1N1 in a hemagglutination inhibition (HI) assay. PBS without virus was used as a positive control: precipitated guinea pig erythrocytes (red circles); PBS with virus alone was used as a negative control: guinea pig erythrocytes did not settle and appeared uniformly red. (C) Time course of addition of compound H1N1-17. H1N1 viruses were pre-incubated with cells (−1 h) for adsorption, and compound H1N1-17 was added at 0 h (endocytosis), 2 h (fusion), and 4 h (uncoating) and 8 h (replication). At 24 h post adsorption, viruses from cellular lysate were harvested and quantified by one-step real time PCR assay. Compound H1N1-17 significantly inhibited endocytosis and fusion at 0 h post adsorption, and antiviral activity of compound H1N1-17 gradually decreased with time. Values are means ± SD ($n = 3$). (D) Inhibition of compound H1N1-17 on hemolysis of guinea pig erythrocytes mediated by H1N1 HA in acidic condition. Values are means ± SD ($n = 3$). *$P < 0.05$, **$P < 0.01$, and ***$P < 0.001$, by one-way Anova (and nonparametric or mixed) in (D).

CPE was observed in Calu3 cells infected with H1N1 virus (Fig. 4A, a4−c4), but not in cells incubated with HA protein (Fig. 4A, a2−c2), indicating no HA proteins caused cytopathy in Calu3 cells. The CPE in H1N1-infected Calu3 cells incubated with HA protein (Fig. 4A, a5−c5) was severe, as it was in Calu3 cells infected with H1N1 virus also (Fig. 4A, a4−c4), suggesting that the HA protein (H1, H3, H8) at experimental concentrations could not counteract the process of virus infection in Calu3 cells. Accordingly, after infection, levels of viral RNAs from cell culture supernatants of Calu3 cells incubated with HA protein scarcely differed from Calu3 cells alone. With treatment of compound H1N1-17, CPE in H1N1-infected Calu3 cells were markedly alleviated (Fig. 4A, a7−c7), and levels of viral RNAs significantly decreased. However, in the presence of H1 protein, the anti-H1N1 activity of H1N1-17 was antagonized by H1 protein, manifested in that CPE aggravated markedly (Fig. 4A, a6), and levels of viral RNAs approached to H1N1-infected Calu3 cells and differed significantly from Calu3 cells treated with H1N1-17. Importantly,

though the activity of compound H1N1-17 was antagonized by H1 protein (Fig. 4A, a6), its anti-H1N1 activity was unaffected by H3 or H8 protein (Fig. 4A, b6 and c6). These results suggested that a direct interaction existed between H1N1-17 and H1, and that this interaction was specific and occurs only between the compound and HA protein of H1N1.

Surface plasmon resonance was used to determine the affinity of compound H1N1-17 towards the HA protein of the H1N1 virus (Fig. 4B). Concentrations of H1N1-17 were two-fold serially diluted (from 1.5625 to 25 μmol/L) to interact with the HA protein of the H1N1 virus (20 μg/mL) on the sensor chip. The K_D value (2.58 μmol/L) confirmed the presence of high affinity between H1N1 HA and H1N1-17.

2.6. Identification of potential action sites of compound H1N1-17 to H1N1 HA

To explore the precise action domains of the compound to H1N1 HA, selection of drug-resistant variants was performed in Calu3 cells using 5 μmol/L (8-fold the EC_{90}) of compound H1N1-17. We continuously passaged H1N1 in Calu3 cells in the presence of compound H1N1-17; the compound-selected resistant strain first appeared after passage five (P5) infection as the CPE deteriorated markedly compared with previous passages (Supporting Information Fig. S4); viruses were isolated in cell culture supernatants in passage six (P6). To confirm and characterize potential mutations generated during selection, viruses grown with or without the compound were collected at P6, amplified in Calu3 cells, and submitted to whole-genome sequencing. This revealed that mutations in two bases in the genome of the resistant strain led to mutations in two amino acids in HA (Supporting Information Fig. S5). Mature HA is a homotrimer (Fig. 5A, PDB ID: 1RU7). Each monomer contains two domains: the membrane-distal receptor binding globular domain (R & E subdomain) that is composed of HA1 residues, and the membrane-proximal helix-rich stalk domain (F subdomain) that is primarily composed of HA2 residues with some HA1 residues. One mutation was in the HA1 sequence, where the residue in position 43 was mutated from L to I, noted HA1 L43I (Fig. 5B). Another mutation was in the HA2 sequence, where the residue in position 109 was mutated from D to G, noted HA2 D109G (Fig. 5B). Both L43 of HA1 and D109 of HA2 were located in the F subdomain of the monomer HA (PDB ID: 6WCR), which is responsible for membrane fusion of the influenza virus and the endosome[19]. We further evaluated the antiviral effect of compound H1N1-17 against the resistant strain. The WT strain remained sensitive to compound H1N1-17 ($EC_{50} = 0.59 \pm 0.24$ μmol/L), while compound H1N1-17 did not inhibit the resistant strain (Fig. 5C). Accordingly, compound H1N1-17 significantly decreased viral proteins of $H1N1^{WT}$ but not viral proteins of $H1N1^{resis}$ and alleviated CPE of $H1N1^{WT}$ infection but not $H1N1^{resis}$ infection in Calu3 cells (Fig. 5D−F). These results demonstrated that compounds H1N1-17 might rely on these two mutation sites to exert its antiviral effect.

To further investigate the correlation between mutation sites and the membrane fusion inhibitory activity of compound H1N1-17, Vero cells were co-transfected with plasmid carrying the encoding sequence of wild-type HA (HA-WT) or HA with mutation sites (HA-Mut: L43I, D109G, or L43I/D109G) and plasmid carrying the encoding sequence of GFP to perform a cell fusion assay. GFP diffused through pores generated by cell membrane fusion, and fluorescence area and intensity will be enhanced. At pH 7.2, Vero cells underwent no fusion, while mutual fusion between Vero cells was triggered by conformational changes of HA at pH 4.8 (the prerequisite for membrane fusion) (Fig. 6). Significant inhibition of H1N1-17 on membrane fusion mediated by HA-WT was observed, while this phenomenon did not occur in membrane fusion mediated by HA-Mut (L43I, D109G, or L43I/D109G). These results suggested that membrane fusion inhibitory activity of compound H1N1-17 strongly depended on these two HA mutation sites.

2.7. Activity of H1N1-17 on lethal H1N1 infection in vivo

To evaluate the *in vivo* efficacy of compound H1N1-17, we performed a murine model challenged with lethal H1N1 (A/PR/8/34) ($n = 6$ for each group). H1N1-infected mice were administrated with compound H1N1-17 at 25 mg/kg/day intraperitoneally from −1 to 10 days post infection (dpi). Compound H1N1-17 resulted in 100% survival, while all mice in the vehicle group died until 12 dpi (Fig. 7A). The weight of mice in the vehicle group declined sharply until all mice had died, while the weight of mice treated with H1N1-17 declined gradually over the first 8 days, but the magnitude of decrease was significantly smaller than that of the vehicle group, after which weight gradually increased to be comparable to initial weight.

We explored the alleviating effect of H1N1-17 on viral infections by detecting viral proteins and viral RNAs in mice lung tissue. Three lung tissue samples were collected in each group at 10 dpi. H1N1-17 effectively alleviated viral infection in lung tissues by significantly reducing levels of viral RNAs and proteins (Fig. 7B and C). H&E staining and Smith lung injury score revealed H1N1-17 to effectively alleviate diffuse alveolar damage caused by viral infection, mainly manifested in the recovery of alveolar wall proliferation and unclear alveolar structure, and reduction in transparent membranes formed by protein and fibrous exudation (Fig. 7D).

2.8. H1N1-17 shows additive to synergistic antiviral activity in vitro with oseltamivir

The U.S. Centers for Disease Control and Prevention (CDC) reported that the resistance level of influenza A virus to oseltamivir has been increasing year by year. The resistance rate of H1N1 to Oseltamivir is approximately 2% to 4%, while in some Asian countries such as Japan and South Korea, it reaches 5% to 7%. For immunocompromised individuals, long-term hospitalized patients, and severe cases, the resistance rate may rise to 5% to 10%, primarily due to prolonged virus exposure and high selective pressure. These phenomena indicate that although the global resistance of influenza viruses to oseltamivir remains at a low level, there is a potential risk of localized outbreaks, which could shorten the lifespan of oseltamivir's clinical use[26]. Combination therapy exploits the chances for better efficacy and reduces development of drug resistance. To guide clinical combination studies, the possibility of mechanistic synergy or antagonism might be assessed using the Prichard−Shipman method in a viral culture model, wherein a checkerboard design is used to generate a 3-dimensional model of drug−drug interactions[27]. We treated Calu3 cells with oseltamivir acid and/or H1N1-17, at concentrations above and below respective EC_{50}s, and then infected these cells with H1N1 viruses. The two inhibitors were tested singly and in combinations such that each concentration of oseltamivir acid was combined with each

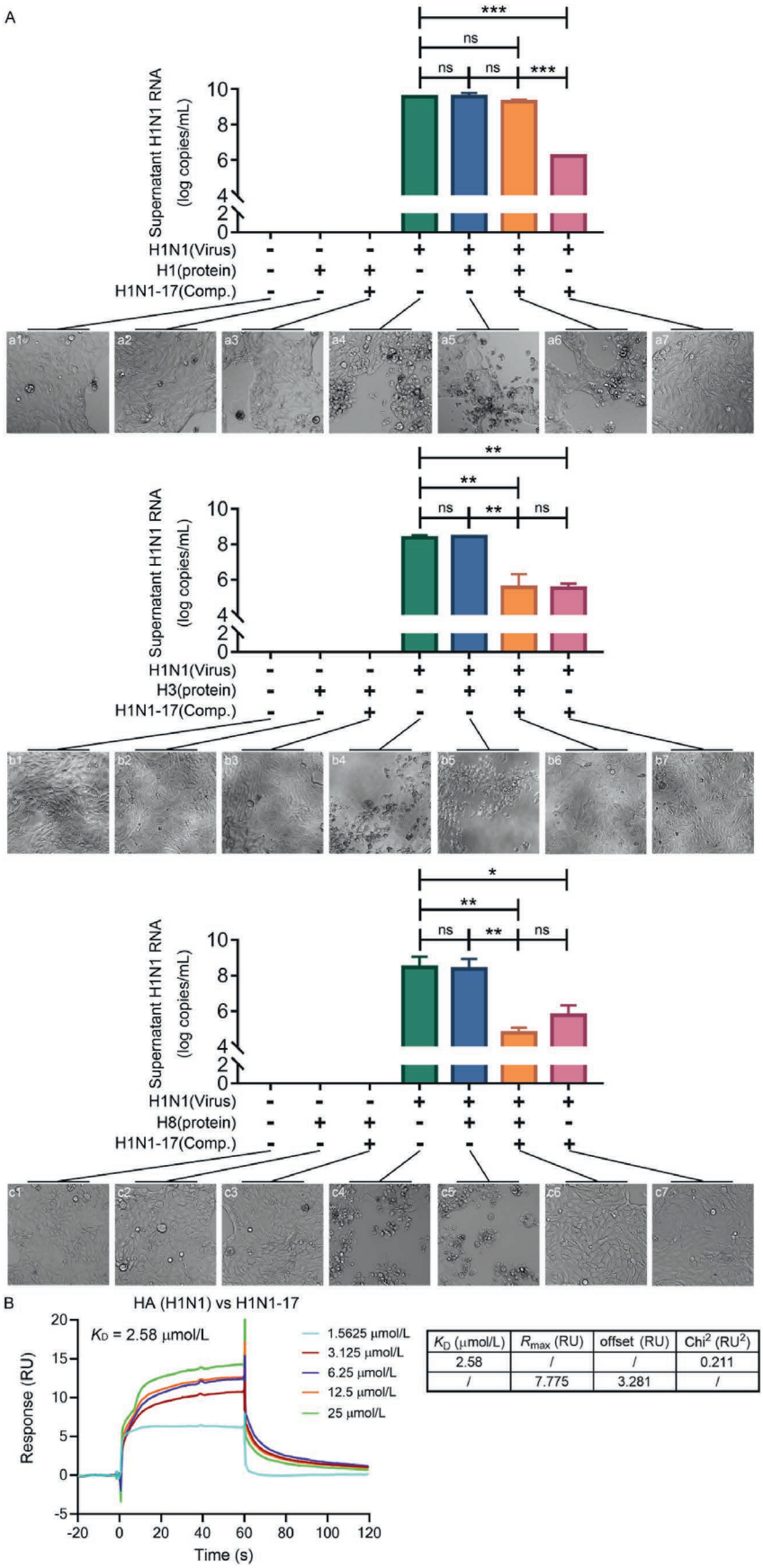

K_D (μmol/L)	R_{max} (RU)	offset (RU)	Chi^2 (RU^2)
2.58	/	/	0.211
/	7.775	3.281	/

concentration of compound H1N1-17 to determine suppressive effects of combination on infection and replication. H1N1-17 exhibited a synergistic antiviral effect in co-treatment with oseltamivir acid (Fig. 8A) with no significant antagonism observed. Results were also analyzed using the median effect/combination index (CI) isobologram equation. For each effect level, CI values were calculated according to the general combination index equation for two inhibitors at 50% inhibition[28]. The CI $<$ 1 indicated that the doses at which H1N1-17 and oseltamivir acid produced a given effect in combination were lower than expected doses from an additive effect (Table 1 and Fig. 8B). These results revealed the mechanistic distinction between H1N1-17 and oseltamivir, which confirmed the potential utility of H1N1-17 for use in combination treatment regimens.

3. Discussion

H1N1 has developed resistance to oseltamivir[29]. Compared with discontinued adamantane drugs, use of oseltamivir will continue as a specific antiviral drug into the immediate future. However, the gradual increase in resistance of H1N1 to oseltamivir suggests that the life span of oseltamivir will be no longer than that of adamantane ($\sim$40 years)[30]. To help patients recover faster and reduce the occurrence of drug resistance, combination regimens that comprise different agents that work together to comprehensively attack influenza virus at different stages in its life cycle have been applied in clinical therapy. Entry inhibitors are a class of directly acting antiviral agent that can supplement current influenza therapies through a combination regimen, and possibly result in a stronger therapeutic effect.

Because of their complex structure and large and rigid surfaces, macrocyclic compounds can bind and modify some target proteins without binding pockets. They thus meet the complexity requirements of current drug targets and have significant advantages in drug development[31]. We designed a novel macrocyclic compound H1N1-17, with potent specific antiviral activity against H1N1, by targeting the stalk domain of the HA to block membrane fusion. The potential binding sites are HA1 L43 and HA2 D109. Sequence alignment analysis revealed varying degrees of amino acid differences near these sites among H1, H5, and H8 subtypes (Supporting Information Fig. S5). These differences may explain why the compound specifically targets H1N1 while exhibiting limited activity against other influenza virus subtypes. Intraperitoneal administration of compound H1N1-17 protected mice challenged with lethal H1N1 from death and weight loss, and effectively alleviated lung injury caused by viral infection−activity comparable with that of oseltamivir phosphate. To guide clinical combination studies, we evaluated the potential for combining H1N1-17 with oseltamivir acid (an active metabolite of oseltamivir). When the net effect of simultaneously inhibiting several targets enhances viral suppression, the use of multiple antiviral drugs in clinical combination regimens is usually beneficial and can accelerate the clearance of infections and prevent the onset of resistance to any one drug. Therefore, the combination of compound H1N1-17 and oseltamivir may result in improved therapeutic effects, reduced drug resistance, and extend the life span of oseltamivir. Because H1N1 has been the main influenza-causing strain this last decade, the synergistic efficacy of compound H1N1-17 and oseltamivir acid is significant for clinical combination therapy.

The main limitation of this study is that compound H1N1-17 has poor water solubility and fails to overcome one of the main drawbacks of macrocyclic compounds, that is the difficulty in achieving oral bioavailability. Therefore, we used intraperitoneal injection as the administration method to evaluate its antiviral activity *in vivo*. Before entering clinical use, compound H1N1-17 needs to undergo pharmacological modification to improve its oral bioavailability. To simultaneously enhance the aqueous solubility and membrane permeability of the macrocycle, two strategic modifications are proposed: the attachment of short polyethylene glycol (PEG) chains, and the replacement of the trifluoromethyl group with a bioisostere such as a cyano (−CN) or sulfonamide ($-SO_2NH_2$) group. These changes are anticipated to reduce the compound's log*P* while preserving its target binding affinity. Then, the biosafety and antiviral effects of compound H1N1-17 need to be further elucidated and studied through preclinical and clinical research.

In conclusion, our study identifies the macrocyclic compound H1N1-17 as a novel HA stalk-targeted inhibitor that blocks membrane fusion, exhibiting potent *in vitro* and *in vivo* anti-H1N1 activity, low toxicity, and synergistic potential with oseltamivir. Its mechanism circumvents antigenic drift limitations of conventional HA head-directed strategies. These findings provide a candidate molecule for combating H1N1 seasonal epidemics and pandemic threats,and lay a scientific foundation for antiviral strategies based on HA stalk domain.

4. Experimental

4.1. Chemicals

The compound pimodivir (CAS: 1629869-44-8), favipiravir (CAS: 259793-96-9), zanamivir (CAS: 139110-80-8), oseltamivir phosphate (CAS: 204255-11-8) and oseltamivir acid (CAS: 187227-45-8) were all purchased from Topscience Co. Ltd. (Shanghai, China). Compounds were dissolved in 100% dimethyl

Figure 4 Direct interaction of compound H1N1-17 with H1N1 HA. (A) Antiviral activity of compound H1N1-17 was specifically antagonized by H1N1 HA in the protein competition assay. Calu3 cells were pre-incubated with H1N1 at 4 °C for adsorption, and then viruses were replaced with compound H1N1-17 incubated with and without HA protein. Viral RNAs from cell culture supernatants were extracted and quantified by one-step real time PCR assay. Values are means ± SD (n = 3). Cell viability and morphology were viewed microscopically using a 10 × objective (scale bar: 100 μm). Calu3 cell morphology: without infection (a1, b1, c1); without infection and incubated with H1 (a2), H3 (b2), and H8 (c2); without infection and treated with compound H1N1-17 that was pre-incubated with H1 (a3), H3 (b3), and H8 (c3); infected with H1N1 (a4, b4, c4); infected with H1N1 and incubated with H1 (a5), H3 (b5), and H8 (c5); infected with H1N1 and treated with compound H1N1-17 that was pre-incubated with H1 (a6), H3 (b6), and H8 (c6); and infected with H1N1 and treated with compound H1N1-17 (a7, b7, c7). (B) Strong interaction of compound H1N1-17 with H1N1 HA determined by surface plasmon resonance assay (K_D = 2.58 μmol/L). The CM5 chip was used for amino coupling fixation of H1N1 HA protein, and compound H1N1-17 was used as the analyte to detect the affinity between H1N1 HA and compound H1N1-17. *P $<$ 0.05, **P $<$ 0.01, and ***P $<$ 0.001, ns indicated no statistical significance, by one-way Anova (and nonparametric or mixed) in (A).

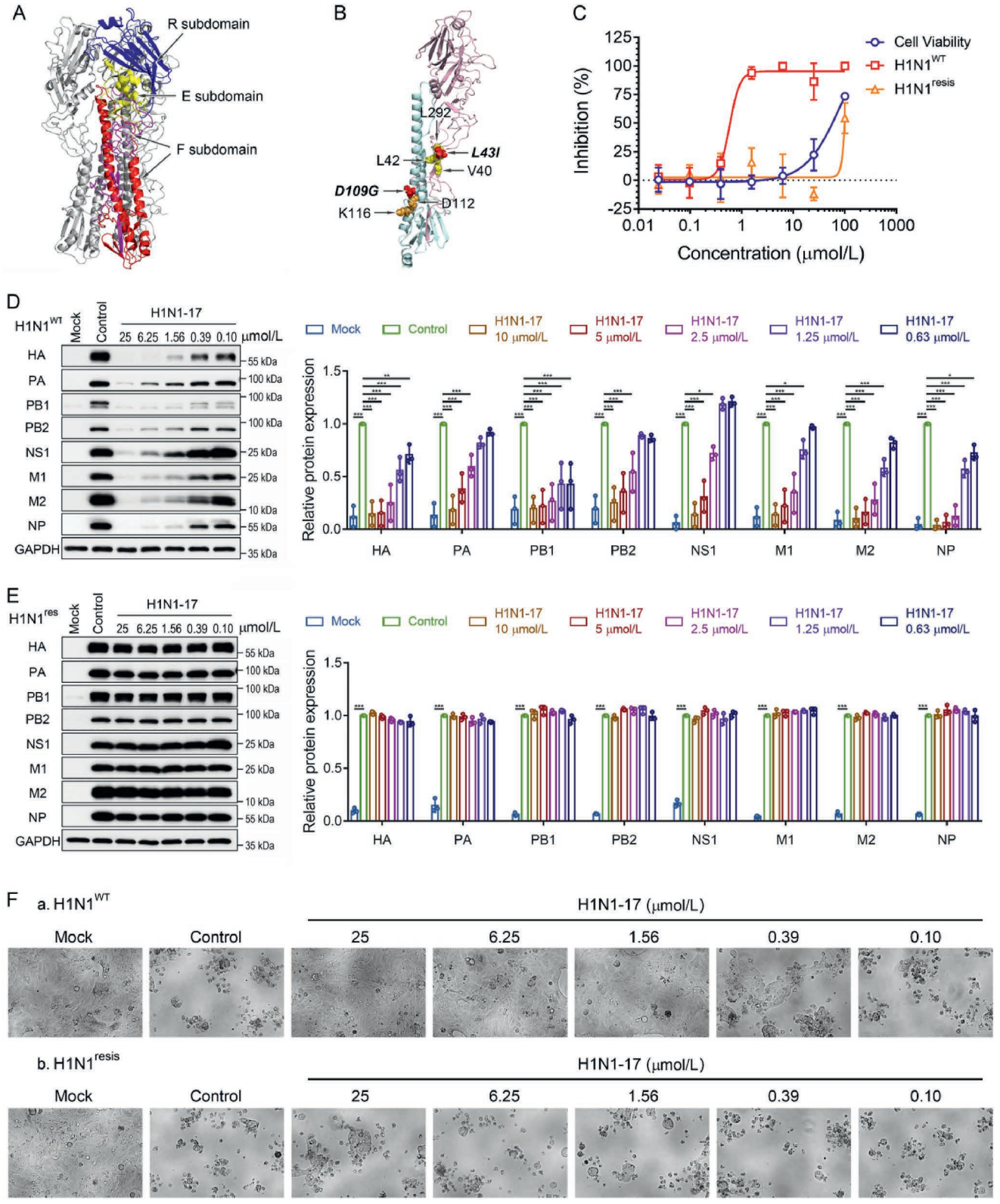

Figure 5 Potential sites of interaction between compound H1N1-17 and H1N1 HA. (A) Structure of the H1N1 (A/PR/8/34) HA trimer (PDB ID: 1RU7) and functional subdomains. Subdomain: blue (R), yellow (E), purple (F, sequence HA1), and red (F, sequence HA2). (B) Resistant mutations (L43I of HA1 and D109G of HA2, red spheres) identified in the H1N1 HA to compound H1N1-17 located in F subdomain. L43I mutation of HA1 located near the interaction sites between CR6261 and H1N1 HA (L42, V40, and L292 of HA1, yellow spheres). The D109G mutation of HA2 was one of the mutation sites that mediated membrane fusion at high pH (D109G, D112, and K116 of HA2, orange spheres). HA1 and HA2 in the structure of H1N1 (A/PR/8/34) HA monomer (PDB ID: 6WCR), light pink and pale cyan, respectively. (C) Compound

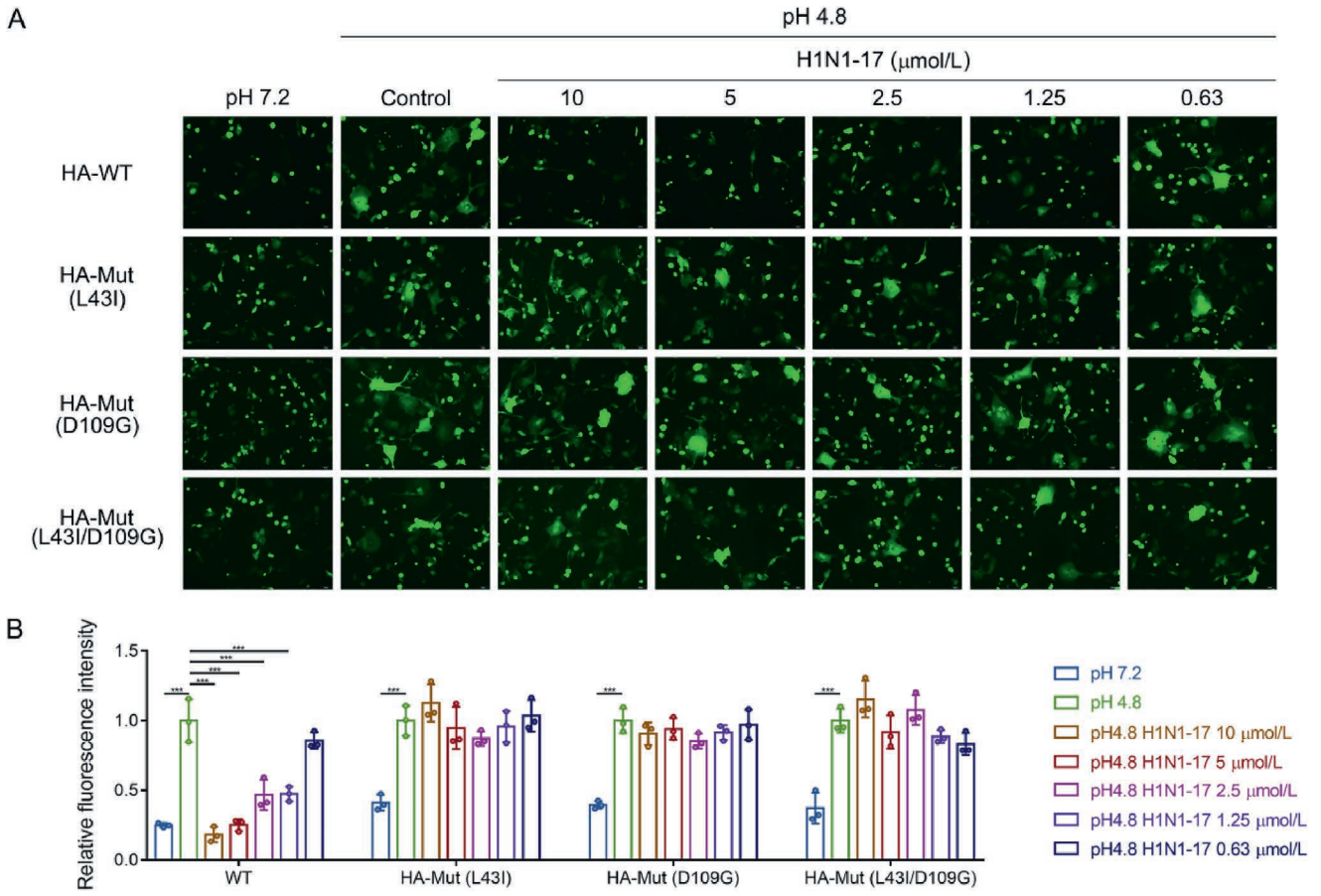

Figure 6 Inhibitory activity of compound H1N1-17 of HA-mediated membrane fusion of Vero cells expressing GFP and HA. Vero cells were co-transfected with plasmid carrying the encoding sequence of wild-type HA (HA-WT) or HA mutants (HA-Mut: L43I, D109G or L43I/D109G) and plasmid carrying the encoding sequence of GFP. The mutual fusion between Vero cells was triggered by conformational changes of HA at pH 4.8 and characterized by the diffusion of GFP in cells (green). Inhibition of H1N1-17 on membrane fusion mediated by HA-WT was observed, while this phenomenon did not occur in membrane fusion mediated by HA mutants that contained one or two drug-resistant mutations (L43I, D109G, or L43I/D109G). (A) Fluorescence images were visualized and photographed using a fluorescence inverted microscope with a 20 × objective (scale bar: 50 μm). (B) Relative fluorescence intensity of fluorescence images in (A). Values are means ± SD ($n = 3$). *$P < 0.05$, **$P < 0.01$, and ***$P < 0.001$, by two-way Anova (or mixed model) in (B).

sulfoxide (Sigma-Aldrich) to obtain 40 mmol/L stock solutions and stored at −30 °C.

*Ethyl 3-((tert-butoxycarbonyl)amino)-2,2-dimethylpropanoate (**2**).* A solution of ethyl 3-amino-2,2-dimethylpropanoate hydrochloride (**1**) (1.0 equiv) and $(Boc)_2O$ (1.5 equiv) in acetone/H_2O (*v*/*v*, 1:1) was treated with $NaHCO_3$ (4.0 equiv) at 0 °C. The mixture was stirred at room temperature for 4 h before being diluted with EtOAc, washed with water and brine, dried over Na_2SO_4, filtered, and concentrated. The residue was purified by flash silica chromatography (0−10% EtOAc in PE) to afford the intermediate **2** (99%) as a colorless oil. ^{1}H NMR (500 MHz, chloroform-*d*) δ 4.98−4.93 (m, 1H), 4.13 (q, $J = 6.9$ Hz, 2H), 3.23 (d, $J = 6.6$ Hz, 2H), 1.43 (s, 9H), 1.26 (t, $J = 7.1$ Hz, 3H), 1.17 (s, 6H). ESI MS *m*/*z*: $[M + H]^+$ 246.2.

*tert-Butyl (3-(methoxy(methyl)amino)-2,2-dimethyl-3-oxopropyl)carbamate (**3**).* To a solution of *N*,*O*-dimethylhydroxylamine hydrochloride (5.0 equiv) in dry THF was added ^{i}PrMgCl (2.0 mol/L in THF, 10 equiv) dropwise at 0 °C. The mixture was stirred for 20 min at 0 °C before being treated with ethyl 3-((*tert*-butoxycarbonyl)amino)-2,2-dimethylpropanoate

H1N1-17 inhibited the multiplication of $H1N1^{WT}$ while $H1N1^{resis}$ was insensitive to compound H1N1-17. $H1N1^{WT}$, the sixth passage of H1N1 in Calu3 cells in the absence of compound H1N1-17; $H1N1^{resis}$, the sixth passage of H1N1 in Calu3 cells in the presence of compound H1N1-17. Values are means ± SD ($n = 3$). (D) Viral proteins of $H1N1^{WT}$ in Calu3 cells significantly decreased with treatment of compound H1N1-17 in Western blot assay. Relative quantification was shown on the right ($n = 3$). Values are means ± SD. (E) Viral proteins of $H1N1^{resis}$ in Calu3 cells were invariable following treatment with compound H1N1-17 in Western blot assay. Relative quantification was shown on the right ($n = 3$). Values are means ± SD. (F) Compound H1N1-17 alleviated the cytopathic effects of $H1N1^{WT}$ but not $H1N1^{resis}$ infection in Calu3 cells. Cell viability and morphology were viewed microscopically using a 10 × objective (scale bar: 100 μm). *$P < 0.05$, **$P < 0.01$, and ***$P < 0.001$, by two-way Anova (or mixed model) in (D) and (E).

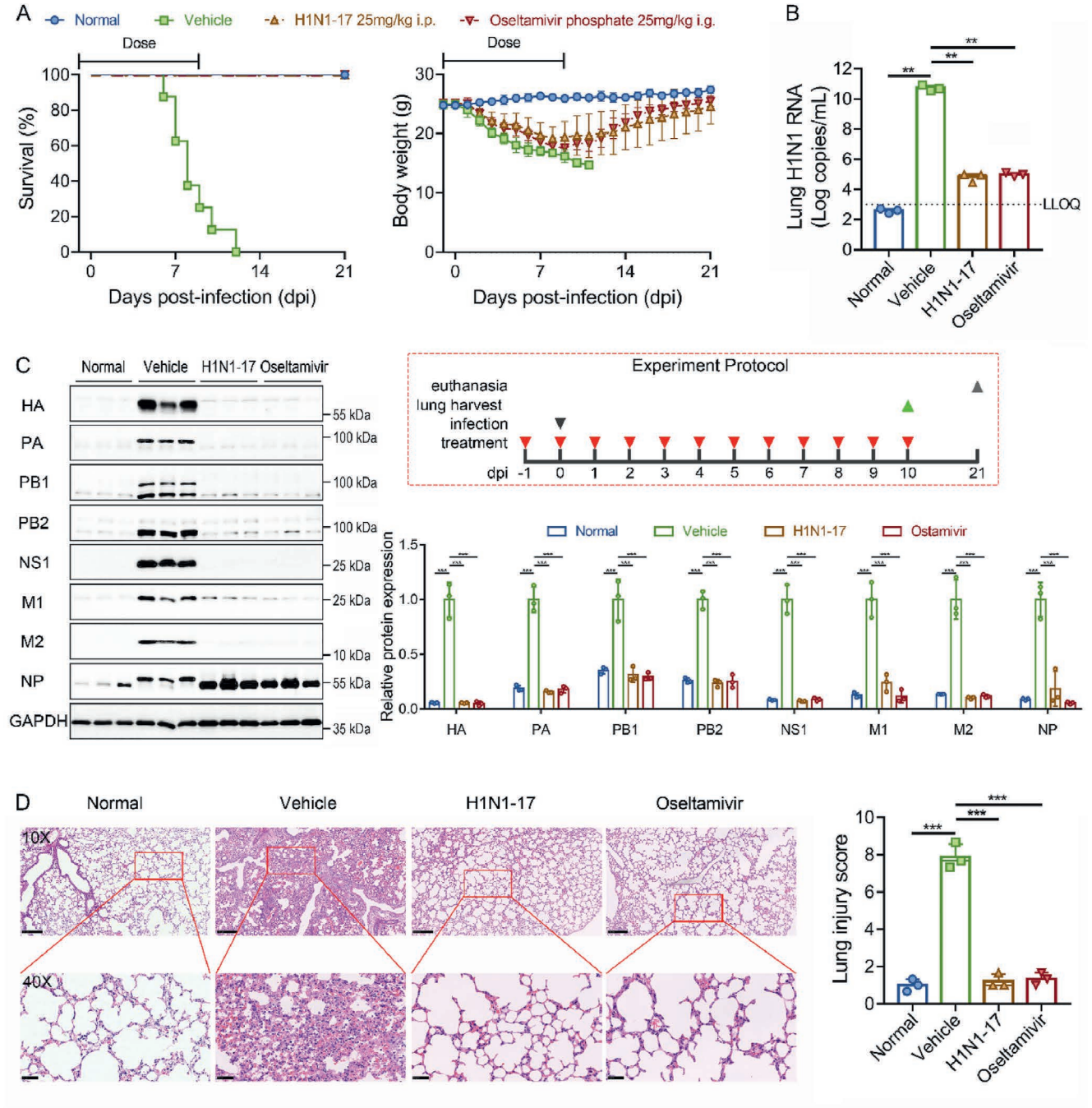

Figure 7 The effect of compound H1N1-17 on mice challenged with lethal H1N1 (A/PR/8/34). Six mice in each group were intranasally inoculated with MLD_{100} of H1N1 (A/PR/8/34) and treated with compound H1N1-17 at 25 mg/kg/day intraperitoneally or oseltamivir phosphate at 25 mg/kg/day intragastrically from −1 to 10 days post infection (dpi). Survival and body weight were monitored daily from −1 to 21 dpi. For pathological analysis, another parallel experiment was performed. Three mice in each group were euthanized on 10 dpi, and lung tissues were isolated. (A) Survival and body weight of H1N1-infected and drug-treated mice. Compound H1N1-17 effectively protected H1N1-infected mice from death and weight loss. Values are means ± SD ($n = 6$). (B) Compound H1N1-17 significantly reduced H1N1 in mice lung tissues. Virus titers in lung tissues were detected by one-step real time PCR assay at 10 dpi. LLOQ, lower limit of quantification: 10^3 copies/mL. Values are means ± SD ($n = 3$). (C) Viral proteins in lung tissues were detected by Western blot assay at 10 dpi. Relative quantification was shown on the right ($n = 3$). Values are means ± SD. (D) Compound H1N1-17 effectively alleviated lung injury caused by viral infection. H1N1-induced pathogenesis was determined by H&E staining at 10 dpi. Smith lung injury score was shown on the right. Values are means ± SD ($n = 3$). $^*P < 0.05$, $^{**}P < 0.01$, and $^{***}P < 0.001$, by two-way Anova (or mixed model) in (C) and one-way Anova (and nonparametric or mixed) in (B) and (D).

Table 1 Combination index (CI) of compound H1N1-17 and oseltamivir acid at 50% inhibition.

Two-chemical combination (nmol/L)		CI_{50} value[a]
Compound H1N1-17 (D)1	Oseltamivir acid (D)2	$2CI_{50}=(D/D_{50})1+(D/D_{50})2$
0.31	324	0.63
1.22	339	0.66
4.88	345	0.69
8.50	313	0.63
19.5	301	0.64
26.1	19.5	0.11
32.6	78.1	0.24
78.1	146	0.49
263	4.88	0.70
313	17.8	0.86

[a] $2CI_{50}$ is the combination index for two chemicals (Compound H1N1-17 and Oseltamivir acid) at 50% inhibition; D is the dose of chemical, D_{50} is the effective dose of a chemical that caused a 50% inhibition of H1N1 replication ($(D_{50})1 = 380$ nmol/L and $(D_{50})2 = 513$ nmol/L).

(**2**) (1.0 equiv) in THF at the same temperature. The mixture was stirred at room temperature for another 2 h. After completion, it was quenched with sat. aq. NH_4Cl and filtered. The filtrate was diluted with EtOAc, washed with water and brine, dried over Na_2SO_4, filtered, and concentrated. The residue was purified by flash silica chromatography (0−20% EtOAc in PE) to yield the intermediate **3** (91%) as a colorless oil. ^{1}H NMR (500 MHz, chloroform-*d*) δ 5.25−5.19 (m, 1H), 3.68 (s, 3H), 3.24 (d, $J = 6.6$ Hz, 2H), 3.17 (s, 3H), 1.42 (s, 9H), 1.25 (s, 6H). ESI-MS *m/z*: $[M + H]^+$ 261.4.

*tert-Butyl (2,2-dimethyl-3-oxohex-5-en-1-yl)carbamate (**4**).* To a solution of *tert*-Butyl (3-(methoxy(methyl)amino)-2,2-dimethyl-3-oxopropyl)carbamate (**3**) (1.0 equiv) in dry THF was added allylmagnesium chloride (2.5 equiv) dropwise at −60 °C. The mixture was stirred at −60 °C for 3 h. After completion, it was quenched with sat. aq. NH_4Cl and filtered. The filtrate was diluted with EtOAc, washed with water and brine, dried over Na_2SO_4, filtered, and concentrated. The residue was purified by flash silica chromatography (0−12% EtOAc in PE) to produce the intermediate **4** (94%) as a colorless oil. ^{1}H NMR (500 MHz, chloroform-*d*) δ 5.93−5.85 (m, 1H), 5.17 (d, $J = 10.3$ Hz, 1H), 5.10 (d, $J = 17.2$ Hz, 1H), 4.93−4.87 (m, 1H), 3.27 (d, $J = 6.8$ Hz, 2H), 3.22 (d, $J = 6.6$ Hz, 2H), 1.41 (s, 9H), 1.16 (s, 6H). ESI-MS *m/z*: $[M + H]^+$ 242.3.

*tert-Butyl (6-hydroxy-2,2-dimethyl-3-oxohexyl)carbamate (**5**).* To a solution of terminal olefin (**4**) (1.0 equiv) in dry THF was added 9-BBN (0.5 mol/L in THF, 1.6 equiv) dropwise at 0 °C. Then, the mixture was stirred at room temperature for 2 h before being quenched with water and $NaBO_3 \cdot 4H_2O$ (10 equiv) was added subsequently. The resulting solution was stirred at room temperature for another 0.5 h. After that, it was diluted with EtOAc, washed with water and brine, dried over Na_2SO_4, filtered, and concentrated. The residue was purified by flash silica chromatography (0−40% EtOAc in PE) to produce the intermediate **5** (84%) as a colorless oil. ^{1}H NMR (500 MHz, chloroform-*d*) δ 4.97−4.92 (m, 1H), 3.62 (t, $J = 6.1$ Hz, 2H), 3.22 (d, $J = 6.7$ Hz, 2H), 2.64 (t, $J = 7.0$ Hz, 2H), 1.81 (p, $J = 6.9$ Hz, 2H), 1.41 (s, 9H), 1.15 (s, 6H). ESI-MS *m/z*: $[M + H]^+$ 260.3.

*tert-Butyl (E)-(6-hydroxy-3-(methoxyimino)-2,2-dimethylhexyl) carbamate (**6**).* A solution of methoxyamine hydrochloride (2.0 equiv) in pyridine was treated with ketone (**5**) (1.0 equiv). The solution was heated at 80 °C for 2 h. After cooling to room temperature, the mixture was concentrated to remove pyridine. Then, it was diluted with EtOAc, washed with sat. aq. NH_4Cl and brine, dried over Na_2SO_4, filtered, and concentrated. The residue was purified by flash silica chromatography (0−30% EtOAc in PE) to yield the intermediate **6** (91%) as a colorless oil. ^{1}H NMR (500 MHz, chloroform-*d*) δ 5.07−5.00 (m, 1H), 3.84 (s, 3H), 3.61 (t, $J = 6.1$ Hz, 2H), 3.23 (d, $J = 6.5$ Hz, 2H), 2.31 (t, $J = 7.8$ Hz, 2H), 1.79 1.70 (m, 2H), 1.43 (s, 9H), 1.09 (s, 6H). ESI-MS *m/z*: $[M + H]^+$ 289.3.

*Ethyl 2-(acetoxymethyl)acrylate (**8**).* A mixture of ethyl 2-(bromomethyl)acrylate (**7**) (1.0 equiv) and NaOAc (3.0 equiv) in MeOH was stirred at 40 °C overnight. The solution was cooled to room temperature and filtered. The filtrate was concentrated and purified by flash silica chromatography (0−4% EtOAc in PE) to give **8** (89%) as a colorless oil. ^{1}H NMR (500 MHz, chloroform-*d*) δ 6.36 (s, 1H), 5.83 (s, 1H), 4.81 (s, 2H), 4.24 (q, $J = 7.0$ Hz, 2H), 2.10 (s, 3H), 1.31 (t, $J = 7.1$ Hz, 3H). ESI-MS *m/z*: $[M + H]^+$ 173.3.

*2-(2-(Ethoxycarbonyl)allyl)-4-(trifluoromethyl)benzoic acid (**10**).* A solution of **8** (1.0 equiv), 4-(trifluoromethyl)benzoic acid (**9**) (3.0 equiv), K_2CO_3 (1.0 equiv), and $[Ru(p\text{-cymene})Cl_2]_2$ (0.2 equiv) in 2,2,2-trifluoroethan-1-ol was stirred at 65 °C overnight. After cooling to room temperature, the mixture was filtered to remove insoluble substance. The filtrate was concentrated and purified by flash silica chromatography (0−5% EtOAc in PE, containing 0.1% TFA) to yield the intermediate **10** (66%) as an off-white solid. ^{1}H NMR (500 MHz, chloroform-*d*) δ 8.01 (d, $J = 8.1$ Hz, 1H), 7.55 (d, $J = 8.2$ Hz, 1H), 7.50 (s, 1H), 6.26 (s, 1H), 5.37 (s, 1H), 4.19 (q, $J = 7.1$ Hz, 2H), 4.07 (s, 2H), 1.26 (t, $J = 7.0$ Hz, 3H). ESI-MS *m/z*: $[M-H]^-$ 301.1.

*Ethyl (E)-2-(2-((6-hydroxy-3-(methoxyimino)-2,2-dimethylhexyl) carbamoyl)-5-(trifluoromethyl)benzyl)acrylate (**11**).* A solution of Boc containing compound (**6**) (1.0 equiv) in DCM was treated with TFA (5.0 equiv). The mixture was stirred at room temperature for 2 h before being concentrated to obtain the amine intermediate without further purification. A solution of carboxylic acid intermediate (**10**) (1.0 equiv) in dry DMF was treated with HATU (1.2 equiv) and DIPEA (6.0 equiv) at 0 °C. Ten minutes later, the obtained amine intermediate (1.0 equiv) dissolved in dry DMF was added. The mixture was stirred at room temperature for 1 h before being diluted with EtOAc, washed with water and brine, dried over Na_2SO_4, filtered, and concentrated. The residue was purified by flash silica

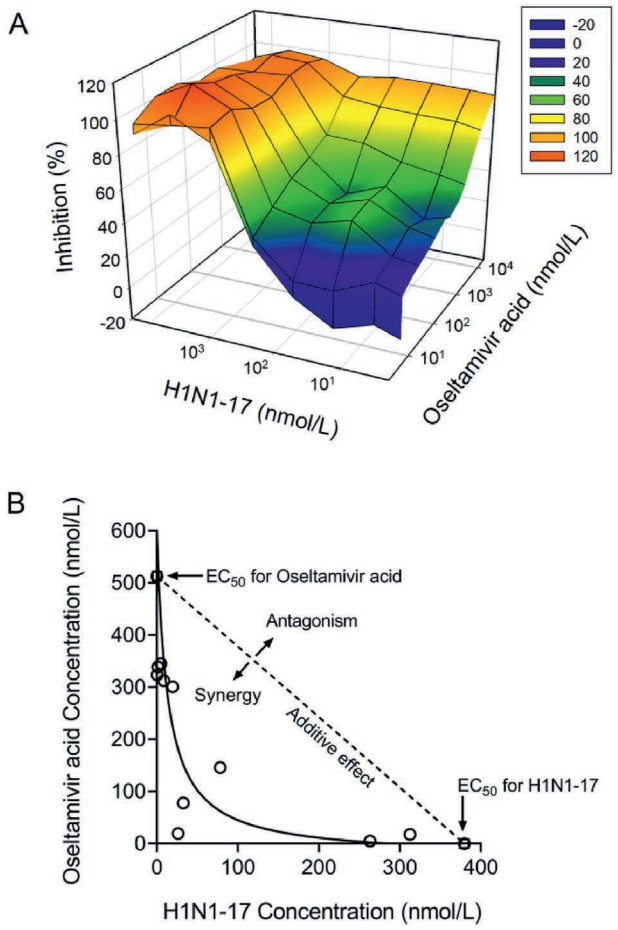

Figure 8 Compound H1N1-17 showed synergistic effect with oseltamivir acid against H1N1. (A) The three-dimensional (3-D) dose-response surface of the combination therapy against H1N1 of compound H1N1-17 and oseltamivir acid. The dose-response surface exhibited a convex shape resembling a flipping sail, especially at an inhibition level of 40%−60% (green). According to the principle of Loewe additivity, the combination therapy against H1N1 of compound H1N1-17 and oseltamivir acid was synergistic. (B) The two-dimensional isobologram of the combination therapy against H1N1 of compound H1N1-17 and oseltamivir acid at the inhibition effect of 50%. By controlling the concentrations of compound H1N1-17 and oseltamivir acid as a constant separately, the EC_{50} against H1N1 of another compound could be calculated to obtain a series of data points, and then the cross-sectional curve in the 3-D dose-response surface at the inhibition level of 50% was obtained, which presented a concave upward curve. According to the principle of Loewe additivity, compound H1N1-17 showed a synergistic effect with oseltamivir acid against H1N1.

chromatography (0−30% EtOAc in PE) to give the intermediate **11** (89%, two steps) as a light-yellow solid. ^{1}H NMR (500 MHz, chloroform-*d*) δ 7.53−7.49 (m, 2H), 7.47 (s, 1H), 7.04 (t, J = 7.4 Hz, 1H), 6.32 (s, 1H), 5.61 (s, 1H), 4.36 (t, J = 7.4 Hz, 2H), 4.15 (q, J = 7.0 Hz, 2H), 3.85 (s, 2H), 3.76 (s, 3H), 3.56 (d, J = 6.6 Hz, 2H), 2.35−2.28 (m, 2H), 1.99−1.92 (m, 2H), 1.26 (t, J = 7.1 Hz, 3H), 1.17 (s, 6H). ESI-MS *m/z*: $[M + H]^+$ 473.6.

*(E)-2-(2-((6-Hydroxy-3-(methoxyimino)-2,2-dimethylhexyl) carbamoyl)-5-(trifluoromethyl)benzyl)acrylic acid (**12**).* To a solution of ester (**11**) (1.0 equiv) in MeOH/H_2O (*v/v*, 1:1) was added NaOH (3.0 equiv) at 0 °C. The mixture was then stirred at 50 °C for 2 h before being concentrated under vacuum to remove MeOH. The resulting residue was diluted with water and extracted with diethyl ether twice. The water layer was acidified with hydrochloric acid at 0 °C to yield a suspension which was filtered and washed with a small amount of EtOH. The filter cake was dried under reduced pressure to provide the corresponding acid **12** (94%) as an off-white solid without further purification. ^{1}H NMR (500 MHz, chloroform-*d*) δ 7.51−7.47 (m, 2H), 7.44 (s, 1H), 7.18 (t, J = 6.3 Hz, 1H), 6.33 (s, 1H), 5.60 (s, 1H), 3.79 (s, 2H), 3.73 (s, 3H), 3.56 (t, J = 6.3 Hz, 2H), 3.53 (d, J = 6.1 Hz, 2H), 2.26 (t, J = 7.7 Hz, 2H), 1.73−1.67 (m, 2H), 1.13 (s, 6H). ^{13}C NMR (126 MHz, chloroform-*d*) δ 169.7, 169.0, 164.4, 140.4, 139.2, 137.5, 131.9 (q, J = 32.5 Hz), 128.7, 128.2, 126.7 (q, J = 3.9 Hz), 123.8 (q, J = 272.2 Hz), 123.6 (q, J = 3.3 Hz), 62.6, 61.6, 47.7, 41.9, 35.3, 29.5, 24.0 (2C), 22.5. HRMS (ESI/QTOF) *m/z*: $[M + H]^+$ calcd for $C_{21}H_{28}F_3N_2O_5$: 445.1945, found 445.1943. HPLC purity: 95.7%.

*(E)-5-(Methoxyimino)-4,4-dimethyl-11-methylene-14-(trifluoromethyl)-3,4,5,6,7,8,11,12-octahydro-2H-benzo[e][1]oxa[8] azacyclotetradecine-1,10-dione (**13**, H1N1-17).* To a solution of acid achieved above (**12**) (1.0 equiv) in dry THF was added Et_3N (5.0 equiv) and 2,4,6-trichlorobenzoyl chloride (1.3 equiv) at 0 °C. The mixture was stirred at room temperature for 1 h. Then, a solution of DMAP (8.0 equiv) in dry THF was treated with the solution above dropwise at 40 °C for 1 h. After that, the resulting solution was stirred at the same temperature for another 30 min before it was concentrated and purified by flash silica chromatography (0−25% EtOAc in PE) to obtain the final compound **13** (H1N1-17) (92%) as an off-white solid. ^{1}H NMR (500 MHz, chloroform-*d*) δ 7.70 (d, J = 8.0 Hz, 1H), 7.54 (d, J = 8.1 Hz, 1H), 7.39 (s, 1H), 6.52 (t, J = 6.5 Hz, 1H), 6.23 (s, 1H), 5.01 (s, 1H), 4.27 (t, J = 5.1 Hz, 2H), 3.82 (s, 2H), 3.65 (s, 3H), 3.56 (d, J = 6.6 Hz, 2H), 2.40 (t, J = 6.2 Hz, 2H), 2.12−2.07 (m, 2H), 1.14 (s, 6H). ^{13}C NMR (126 MHz, chloroform-*d*) δ 167.7, 166.3, 162.9, 140.8, 140.4, 134.1, 131.8 (q, J = 32.7 Hz), 130.7, 127.9 (q, J = 3.8 Hz), 126.5, 124.2 (q, J = 3.5 Hz), 123.7 (q, J = 272.3 Hz), 66.2, 61.4, 47.3, 42.7, 35.0, 25.6, 24.4 (2C), 24.1. HRMS (ESI/QTOF) *m/z*: $[M + H]^+$ calcd for $C_{21}H_{26}F_3N_2O_4$: 427.1839, found 427.1838. HPLC purity: 99.1%.

4.2. Cells

MDCK (NBL2) (Madin-Darby Canine Kidney) cells were obtained from the American Type Culture Collection (ATCC, CCL-34) and were cultured in Dulbecco's Modified Eagle Medium (DMEM; Gibco) supplemented with 10% fetal bovine serum (FBS; Gibco) and 25 mmol/L HEPES (Gibco) at 37 °C in a 5% CO_2 incubator[32]. Calu3 cells were obtained from ATCC (HTB-55) and were cultured in RPMI 1640 (Gibco) supplemented with 10% FBS (Hyclone) at 37 °C in a 5% CO_2 incubator[33]. 293T cells were obtained from ATCC (CRL-3216) and were cultured in DMEM supplemented with 10% FBS (Hyclone) at 37 °C in a 5% CO_2 incubator.

4.3. Influenza viral strains

Influenza virus H1N1 (A/Puerto Rico/8/34, A/California/07/2009 pdm09, A/WS/33, A/FM/1/47), H3N2 (A/Hong Kong/8/68, A/California/2/2014) and influenza B virus (B/Taiwan/2/62) were obtained from ATCC (VR-1469, VR-1894, VR-1520, VR-97, VR-1679 and VR-1938 and VR-1735). DMEM containing 2 μg/mL

N-tosyl-L-phenylalanyl chloromethyl ketone (TPCK) -treated trypsin (Sigma) was used for virus propagation in MDCK cells. 50% tissue culture infectious dose (TCID50) titer was determined by serial titration of viruses on MDCK cells and calculated by Reed-Muench method using GraphPad Prism[34].

4.4. Cytotoxicity assay

The cytotoxicity of compound H1N1-17 was evaluated by adenosine triphosphate (ATP) assay[35]. MDCK cells were seeded into 96-well plates at a density of 1×10^4 cells per well for 24 h. Thereafter, compound H1N1-17 at serially diluted concentrations were added. After a 3-days culture, the cytotoxicity of compound H1N1-17 was determined by CellTiter-Lumi™ Steady Plus Luminescent Cell Viability Assay Kit (Beyotime Biotechnology). In brief, the 3-days cultured MDCK cells were incubated with 100-μL ATP detection reagent and 100-μL phosphate buffered saline (PBS), and the intensity of chemiluminescence which was directly proportional to the number of viable cells was measured by a bioluminometer. Fifty percent cytotoxic concentration value (CC_{50}) was calculated by Reed-Muench method using GraphPad Prism.

4.5. In vitro antiviral activity assay

To measure the antiviral activity of compound H1N1-17, MDCK cells were seeded into 96-well plates at a density of 1×10^4 cells per well. On the following day, compound H1N1-17 at serial dilutions were added 2 h before H1N1 or H3N2 viruses at 0.025 TCID50 and 2 μg/mL TPCK-treated trypsin were added. After a 3-days culture, viral RNAs from cell culture supernatants were extracted using the Qiasymphony Nucleic acid extraction and purification kits (Qiagen). The absolute quantification of viral RNAs was measured by one-step real time PCR assay, and serial dilutions of synthetic RNAs were used for establishing standard curve[23]. 50% maximal effective concentration value (EC_{50}) was calculated by Reed-Muench method using GraphPad Prism.

4.6. Viral cytopathic effect (CPE) assay

MDCK or Calu3 cells were seeded into 6-well plates at a density of 3×10^5 cells per well. The next day, compound H1N1-17 at serial dilutions were added 2 h before H1N1 or H3N2 viruses at 2.5 TCID50 and 2 μg/mL TPCK-treated trypsin were added. The well containing no virus was defined as mock, and the well containing viruses alone was defined as control. After a 3-days culture, the cell viability and morphology were viewed using a microscope with a 10 × objective (Olympus, Japan).

4.7. Western blot assay

MDCK or Calu3 cells were seeded into 6-well plates at a density of 3×10^5 cells per well overnight. Next day, compound H1N1-17 at serial dilutions were added 2 h before H1N1 or H3N2 viruses at 0.025 TCID50 were added. Besides, MDCK cells were also needed to be treated with 2 μg/mL TPCK-treated trypsin. After a 3-days treatment, viral proteins were separated using sodium dodecyl sulfate polyacrylamide gel electrophoresis (SDS-PAGE) and detected by specific antibodies which targeted hemagglutinin (HA; GTX127357), polymerase acid protein (PA; GTX118991), polymerase basic protein 1 (PB1; GTX125923), polymerase basic protein 2 (PB2; GTX125926), nonstructural protein 1 (NS1; GTX125990), matrix protein 1 (M1; GTX125928), matrix protein 2 (M2; GTX125951), and nucleoprotein (NP; ab128193), respectively. Relative protein expression was analyzed using Image J and Graphpad Prism.

4.8. Immunofluorescence assay

MDCK or Calu3 cells were cultured in 12-well plates, and fused to grow at 37 °C overnight. Next day, compound H1N1-17 at serial dilutions were added 2 h before H1N1 or H3N2 viruses at 0.025 TCID50 were added. Besides, MDCK cells were also needed to be treated with 2 μg/mL TPCK-treated trypsin. The well containing no virus was defined as mock, and the well containing viruses alone was defined as control. After a 3-days treatment, cell culture supernatant was discarded, and cells were washed with PBS and fixed with 4% paraformaldehyde at room temperature for 10 min. Cells were then permeabilized with 1% Triton X-100 at room temperature for 15 min, washed with PBS, and then blocked with 3% BSA for 1 h. Then, cells were stained with fluorescein isothiocyanate (FITC)-labeled anti-NP antibody (ab210526) for the NP protein of H1N1 at room temperature for 1 h. After that, cell nuclei were stained with 2-(4-amidinophenyl)-6-indolecarbamidine dihydrochloride (DAPI; Sigma). The fluorescence images were visualized and photographed using a fluorescence inverted microscope with a 10 × objective (Olympus, Japan). Relative fluorescence intensity was analyzed using Image J and GraphPad Prism.

4.9. Time-of-addition assay

Calu3 cells were seeded into 96-well plate at a density of 1×10^4 cells per well overnight. Next day, compound H1N1-17 at serial dilutions and H1N1 viruses at 0.025 TCID50 were added. The time when viruses were added was defined as 0 h. Compound H1N1-17 at serial dilutions were added at −2, 0, 2, 4, 8 and 24 h. At 48 h, viral RNAs from cell culture supernatants were extracted and determined by one-step real time PCR assay.

4.10. Production of pseudo-type viruses and entry inhibition assay

A pseudo-type virus expressing luciferase (Luc) was constructed and expression of which in host cells would be driven by successful entry of pseudo-type viruses, based on the modified defective HIV-1 backbone for entry inhibition assay[36]. In brief, the coding sequence of viral proteins were obtained from the published viral genomes (GenBank: NC_002017 for HA of H1N1, GenBank: AF046098.1 for HA of H5N1, GenBank: NC_002018.1 for NA of H1N1; GenBank: HQ853339.1 for HA of H1N2, and GenBank: HQ853344.1 for NA of H1N2). An optimized coding sequence was chemically synthesized and cloned into the pCAG vector, which was verified by sequencing. 293T cells were co-transfected with pCAG-HA (H1N1) and pCAG-NA (N1), or pCAG-HA (H5N1) and pCAG-NA (N1), or pCAG-HA (H1N2) and pCAG-NA (N2) plasmids plus HIV-1 backbone vector pNL4-3. Luc. R-E− plasmid using X-tremeGENE DNA HP Transfection Reagent (Roche). The third day post transfection, viruses from cell culture supernatants were harvested and filtered with 0.45 μm membrane. The entry inhibition assay was performed as previously described[37].

4.11. Neuraminidase inhibition (NI) assay

NA-XTD™ Influenza Neuraminidase Assay Kit (Thermo Fisher Scientific) was used to measure the inhibition of neuraminidase activity by compound H1N1-17. Briefly, in 96-well NA-XTD detection microplates, viruses at desired dosage (10-fold dilution for H1N1 and stock solution for H3N2) in a 25-μL volume were incubated with compound H1N1-17 or zanamivir at serially diluted concentrations in the same volume at 37 °C for 20 min. The testing plates contained mock (NA-XTD assay buffer only) and control (NA-XTD assay buffer and viruses). Then, NA-XTD substrate in a 25-μL volume was added and incubated with viruses and compounds at room temperature for 30 min, followed by NA-XTD accelerator in a 60-μL volume was added. The intensity of chemiluminescence which was directly proportional to the neuraminidase activity was measured by a bioluminometer.

4.12. Hemagglutination inhibition (HI) assay

In 96-well plates, 4 hemagglutination units (HAU) of H1N1 viruses in a 25-μL volume were incubated with an equal volume of compound at 4-fold-serial dilutions from 100 to 0.0001 μmol/L or with 25-μL PBS as a negative control at room temperature for 30 min. PBS without virus was used as a positive control. Then, 50-μL of 0.5% (*v*/*v* in PBS) of guinea pig erythrocytes (Sbjbio life Sciences) were added and incubated at room temperature for 40 min. Guinea pig erythrocytes in positive wells sedimented and formed red buttons, whereas negative wells had an opaque appearance with no sedimentation.

4.13. Time-of-addition assay within single-round life cycle of H1N1

Calu3 cells were seeded into 96-well plate at a density of 2×10^4 cells per well overnight. Next day, cells were pre-incubated with 2.5 TCID50 H1N1 viruses at 4 °C for 1 h for adsorption. Compound H1N1-17 at serial dilutions were added at 0 (endocytosis and fusion), 2 (uncoating), 4 and 8 h after the temperature rose to 37 °C. At 24 h, intracellular viral RNAs were extracted and determined by one-step real time PCR assay.

4.14. Hemolysis inhibition assay

100-μL compound H1N1-17 with 4-fold-serial dilutions from 100 to 0.006 μmol/L in PBS and an equal volume of 2^6 HAU of H1N1 viruses were added to the deep-well plate, and the mixture was incubated at 37 °C for 1 h[38]. Then, 2% (*v*/*v* in PBS) of guinea pig erythrocytes in 200-μL were added, and the mixture was incubated at 37 °C for 20 min. Thereafter, sodium acetate buffer (0.1 mol/L) at pH 4.6 in a 100-μL volume was added, and the mixture was incubated at 37 °C for 30 min. The deep-well plate was centrifugated at 1000×*g* at 4 °C for 6 min. Then, the supernatant in a 300-μL volume was pipetted, and concentration of the hemoglobin in the supernatant which was directly proportional to the degree of hemolysis was determined by measuring the absorbance at 540 nm using a bioluminometer.

4.15. Protein competition inhibition assay

Hemagglutinins were purchased from MCE (H1, HY-P76447; H3, HY-P77026; H8, HY-P77034). Calu3 cells were seeded into 96-well plates at a density of 1×10^4 cells per well overnight. Next day, cells were incubated with H1N1 viruses at 2.5 TCID50 at 4 °C for 1 h for adsorption. Afterwards, 1 μmol/L H1N1-17 with or without 0.25 μmol/L hemagglutinins was added to well and the plate was transferred to a 37 °C incubator. After a 3-days treatment, the cell viability and morphology were viewed using a microscope with a 10 × objective. Besides, viral RNAs from cell culture supernatants were extracted and determined by one-step real time PCR assay.

4.16. Surface plasma resonance (SPR) assay

A SPR biosensor instrument GE BiacoreT200 (GE, USA) was used to conduct the SPR assay. A carboxymethylated dextran sensor (CM5) chip was used to immobilize H1N1 HA protein through amino group coupling, and compound H1N1-17 at serial dilutions (25, 12.5, 6.25, 3.125 and 1.5625 μmol/L) dissolved in PBS-P^+ buffer flowed over the sensor chip surface with a rate of 50 μL/min at 25 °C. The binding and dissociation time were both 60 s. The sensor chip surface was then regenerated by washing with PBS-P^+ buffer with a rate of 30 μL/min for 30 s. As control, the reference channel without H1N1 HA was used to rectify nonspecific binding and bulk refractive index change. The results were analyzed using the BiacoreT200 SPR evaluation software and the sensing diagram of combination was drawn based on these data.

4.17. Production and identification of H1N1-17-resistant mutant H1N1 virus

The confluent Calu3 cell monolayers pretreated with compound H1N1-17 (5 μmol/L, 8-fold the EC_{90}) were infected with H1N1 viruses at 2.5 TCID50. One hour after infection, H1N1 viruses were washed out and replaced with RPMI 1640 containing compound H1N1-17 (5 μmol/L). After a 3-days treatment, viruses were harvested and subjected to the successive passages until the appearance of a severe CPE (higher than 80%) observed with the microscope (10 × objective), and the viruses from cell culture supernatant of this passage were harvested and identified with whole genome sequencing. Afterwards, resistant mutant viruses were tested and verified using the routine methods containing *in vitro* antiviral activity assay, viral cytopathic effect (CPE) assay, and Western blot assay.

4.18. Cell fusion assay

The confluent Vero cell monolayers cultured in 6-well plates were co-transfected with pCAG-HA (HA-WT (H1), HA-Mut (L43I), HA-Mut (D109G) or HA-Mut (L43I/D109G)) and pEGFP-N1 (Sangon Biotech) using X-tremeGENE DNA HP Transfection Reagent (Roche), and then were treated with 5 μg/mL TPCK-treated trypsin at 37 °C for 10 min[38]. Thereafter, the DMEM medium with or without compound H1N1-17 was added to inactivate the TPCK-treated trypsin for 4 h. Then, the cells were treated with PBS-HCl (acidic PBS adjusted to pH 4.8 using hydrochloric acid) at 37 °C for 3 min. After washing the cells with PBS, the fresh medium containing 2 μg/mL TPCK-treated trypsin and compound H1N1-17 was added and cultured at 37 °C for 24 h to enable GFP to spread through the pores generated by cell fusion. The fluorescence images were visualized and photographed using a fluorescence inverted microscope with a 20 × objective. Relative fluorescence intensity was analyzed using Image J and Graphpad Prism.

4.19. Drug combination assay

Calu3 cells were seeded into 96-well plates at a density of 1×10^4 cells overnight. On the next day, the compound H1N1-17 and oseltamivir acid were tested both singly and in combinations at 4-fold-serial dilutions in the form of orthogonality, and then H1N1 viruses at 0.025 TCID50 were added into corresponding wells. After a 3-days culture, viral RNAs from cell culture supernatants were extracted and quantified by one-step real time PCR assay. The results were analyzed according to the principle of Loewe additivity, and the three-dimensional dose-response surface and two-dimensional isobologram were used to visualize the drug combination[28,39]. For each effect level, combination index (CI) values were then calculated according to the general combination index equation for two-chemical combination, where $2(CI)_{50}$ is the combination index for two chemicals at 50% inhibition.

4.20. In vivo antiviral activity assay

All *in vivo* experiments were conducted in accordance with the National Institute of Health Guide for Care and Use of Laboratory Animals. Animal work was approved by the Bioethics Committee of the Shanghai Institute of Materia Medica.

BALB/c male mice (6−8 weeks old) purchased from SLRC laboratory (Shanghai, China) were intranasally inoculated with MLD_{100} (100% mouse lethal dose) of H1N1(A/Puerto Rico/8/34)[40]. Dosing formulations for compounds were freshly prepared by dissolving H1N1-17 in DMSO/EtOH/PEG300/0.9% NaCl (5/5/40/50, *v*/*v*/*v*/*v*), or oseltamivir phosphate in CMC-Na/H_2O (0.5%, *m*/*v*) at 2.5 mg/mL. H1N1-17 (10 mL/kg) was injected intraperitoneally (i.p.), and oseltamivir phosphate (10 mL/kg) was administered intragastrically (i.g.) once a day. The drug treatments were given one day before (prophylactic) virus challenge and continued until 10 days post infection (dpi). The body weights (g) and survival (%) of mice were monitored daily, and the living mice were euthanized until body weights of mice rebounded to be almost equivalent to the initial body weight (21 dpi).

For pathological analysis, another parallel experiment was performed. At 10 days post-infection (10 dpi), three mice in each group were euthanized, and lung tissues were collected. Part of tissue was used for analysis of gene by one-step real time PCR assay and protein expression by Western blot assay. Another part of tissue was fixed with 4% paraformaldehyde (PFA), preparing for tissue sections. Tissue sections were stained with hematoxylin and eosin (H&E), dried and observed under a light microscope (Olympus, Japan). The degree of lung injury caused by viral infection was scored based on the Smith lung injury score. In brief, semi-quantitative analysis was performed on pulmonary edema, alveolar and interstitial inflammation, alveolar and interstitial bleeding, atelectasis and hyaline membrane formation on a scale of 0−4 points. No damage: 0, lesion range <25%: 1, lesion range 25% to 50%: 2, lesion range 50% to 75%: 3, lesion full field of view: 4. The total lung injury score is the sum of the above items. Each tissue was observed for 3 fields (40 × objective), and the average value was taken and data was analyzed by GraphPad Prism.

4.21. Statistical analysis

Data was analyzed and graphed using Microsoft Excel and GraphPad Prism and presented as means ± SD from at least 3 independent experiments. The statistical significance was determined by one-way Anova (and nonparametric or mixed) or two-way Anova (or mixed model) for multiple groups. A P value < 0.05 was considered statistically significant. Cell morphology and fluorescence were monitored and captured by a fluorescence inverted microscope (10 × objective: scale bar = 100 μm, 20 × objective: scale bar = 50 μm) and graphed by Adobe Photoshop. Relative protein expression and fluorescence intensity were analyzed by Image J.

Acknowledgments

This study was supported by the Strategic Priority Research Program of the Chinese Academy of Sciences, Grant No. XDA 0530303, and National Natural Science Foundation of China (NSFC) (No. 82373708 & No. 22171275, China). The authors would like to thank Prof. Wanchao Yin (Shanghai Institute of Materia Medica, Chinese Academy of Sciences, Shanghai, China) for structural analysis of HA protein.

Author contributions

Ying Gong and Tongyu Bi performed experiments. Ying Gong and Fuling Xiao performed data analysis. Dandan Xu and Han Wang synthesized compounds. Xun Zhang synthesized some macrocyclic precursors. Peng Yu purified the HA protein. Xiaoqian Yang helped with animal studies. Jianping Zuo provided critical comments on the study. Li Yang, Weibo Yang and Xiankun Tong drafted the paper and designed the overall study.

Conflicts of interest

The authors declare no conflicts of interest.

Appendix A. Supporting information

Supporting information to this article can be found online at https://doi.org/10.1016/j.apsb.2026.02.003.

References

1. Godoy P, Soldevila N, Martínez A, Godoy S, Jané M, Torner N, et al. Effectiveness of influenza vaccination and early antiviral treatment in reducing pneumonia risk in severe influenza cases. *Vaccines (Basel)* 2024;**12**:173.
2. Kumari R, Sharma SD, Kumar A, Ende Z, Mishina M, Wang Y, et al. Antiviral approaches against influenza virus. *Clin Microbiol Rev* 2023;**36**:e0004022.
3. Glubokova EA, Leneva IA, Kartashova NP, Falynskova IN, Tikhov RM, Kuznetsov NY. Efficacy of (*R*)-6-adamantane-derivatives of 1,3-oxazinan-2-one and piperidine-2,4-dione in the treatment of mice infected by the A/California/04/2009 influenza virus. *Acta Naturae* 2021;**13**:116−25.
4. Wang C, Takeuchi K, Pinto LH, Lamb RA. Ion channel activity of influenza A virus M2 protein: characterization of the amantadine block. *J Virol* 1993;**67**:5585−94.
5. Pielak RM, Oxenoid K, Chou JJ. Structural investigation of rimantadine inhibition of the AM2-BM2 chimera channel of influenza viruses. *Structure* 2011;**19**:1655−63.
6. Varghese JN, Laver WG, Colman PM. Structure of the influenza virus glycoprotein antigen neuraminidase at 2.9 A resolution. *Nature* 1983;**303**:35−40.
7. Elliott M. Zanamivir: from drug design to the clinic. *Philos Trans R Soc Lond B Biol Sci* 2001;**356**:1885−93.

8. Palomba E, Castelli V, Renisi G, Bandera A, Lombardi A, Gori A. Antiviral treatments for influenza. *Semin Respir Crit Care Med* 2021; **42**:859−72.
9. Palese P, Compans RW. Inhibition of influenza virus replication in tissue culture by 2-deoxy-2,3-dehydro-*N*-trifluoroacetylneuraminic acid (FANA): mechanism of action. *J Gen Virol* 1976;**33**:159−63.
10. Dufrasne F. Baloxavir marboxil: an original new drug against influenza. *Pharmaceuticals* 2021;**15**:28.
11. Jia H, Hu L, Zhang J, Huang X, Jiang Y, Dong G, et al. Recent advances of phenotypic screening strategies in the application of anti-influenza virus drug discovery. *RSC Med Chem* 2024;**15**:70−80.
12. Samji T. Influenza A: understanding the viral life cycle. *Yale J Biol Med* 2009;**82**:153−9.
13. Cho KJ, Lee JH, Hong KW, Kim SH, Park Y, Lee JY, et al. Insight into structural diversity of influenza virus haemagglutinin. *J Gen Virol* 2013;**94**:1712−22.
14. Skehel JJ, Wiley DC. Receptor binding and membrane fusion in virus entry: the influenza hemagglutinin. *Annu Rev Biochem* 2000;**69**: 531−69.
15. Li F, Ma C, Wang J. Inhibitors targeting the influenza virus hemagglutinin. *Curr Med Chem* 2015;**22**:1361−82.
16. Shen X, Zhang X, Liu S. Novel hemagglutinin-based influenza virus inhibitors. *J Thorac Dis* 2013;**5**(Suppl 2):S149−59.
17. Yang J, Li M, Shen X, Liu S. Influenza A virus entry inhibitors targeting the hemagglutinin. *Viruses* 2013;**5**:352−73.
18. Russell CJ, Hu M, Okda FA. Influenza hemagglutinin protein stability, activation, and pandemic risk. *Trends Microbiol* 2018;**26**: 841−53.
19. Gamblin SJ, Vachieri SG, Xiong X, Zhang J, Martin SR, Skehel JJ. Hemagglutinin structure and activities. *Cold Spring Harb Perspect Med* 2021;**11**:a038638.
20. Hussein AFA, Cheng H, Tundup S, Antanasijevic A, Varhegyi E, Perez J, et al. Identification of entry inhibitors with 4-aminopiperidine scaffold targeting group 1 influenza A virus. *Antivir Res* 2020;**177**: 104782.
21. Du R, Cheng H, Cui Q, Peet NP, Gaisina IN, Rong L. Identification of a novel inhibitor targeting influenza A virus group 2 hemagglutinins. *Antivir Res* 2021;**186**:105013.
22. Liu C, Hu L, Dong G, Zhang Y, Ferreira da Silva-Júnior E, Liu X, et al. Emerging drug design strategies in anti-influenza drug discovery. *Acta Pharm Sin B* 2023;**13**:4715−32.
23. Wang H, Li Z, Chen X, Wong JJ, Bi T, Tong X, et al. Multicomponent coupling and macrocyclization enabled by Rh(III)-catalyzed dual C−H activation: macrocyclic oxime inhibitor of influenza H1N1. *Chem* 2023;**9**:607−23.
24. Suzuki T, Takahashi T, Guo CT, Hidari KI, Miyamoto D, Goto H, et al. Sialidase activity of influenza A virus in an endocytic pathway enhances viral replication. *J Virol* 2005;**79**:11705−15.
25. Tang G, Lin X, Qiu Z, Li W, Zhu L, Wang L, et al. Design and synthesis of benzenesulfonamide derivatives as potent anti-influenza hemagglutinin inhibitors. *ACS Med Chem Lett* 2011;**2**:603−7.
26. Tandel K, Sharma S, Dash PK, Parida M. Oseltamivir-resistant influenza A(H1N1)pdm09 virus associated with high case fatality, India 2015. *J Med Virol* 2018;**90**:836−43.
27. Sühnel J. Comment on the paper: a three-dimensional model to analyze drug−drug interactions: Prichard, M.N. and Shipman, C., Jr. *Antivir Res* 1990;**14**:181−206. Antiviral Res 1992;17:91-98.
28. Foucquier J, Guedj M. Analysis of drug combinations: current methodological landscape. *Pharmacol Res Perspect* 2015;**3**:e00149.
29. Zhang W, Xu H, Guan S, Wang C, Dong G. Frequency and distribution of H1N1 influenza A viruses with oseltamivir-resistant mutations worldwide before and after the 2009 pandemic. *J Med Virol* 2022;**94**:4406−16.
30. Lampejo T. Influenza and antiviral resistance: an overview. *Eur J Clin Microbiol Infect Dis* 2020;**39**:1201−8.
31. Yudin AK. Macrocycles: lessons from the distant past, recent developments, and future directions. *Chem Sci* 2015;**6**:30−49.
32. Luo R, Lv C, Wang T, Deng X, Sima M, Guo J, et al. A potential Chinese medicine monomer against influenza A virus and influenza B virus: isoquercitrin. *Chin Med* 2023;**18**:144.
33. Dissanayake TK, Yan B, Ng AC, Zhao H, Chan G, Yip CC, et al. Differential role of sphingomyelin in influenza virus, rhinovirus and SARS-CoV-2 infection of Calu-3 cells. *J Gen Virol* 2021;**102**:001593.
34. Cresta D, Warren DC, Quirouette C, Smith AP, Lane LC, Smith AM, et al. Time to revisit the endpoint dilution assay and to replace the TCID50 as a measure of a virus sample's infection concentration. *PLoS Comput Biol* 2021;**17**:e1009480.
35. Didamson OC, Chandran R, Abrahamse H. Aluminium phthalocyanine-mediated photodynamic therapy induces ATM-related DNA damage response and apoptosis in human oesophageal cancer cells. *Front Oncol* 2024;**14**:1338802.
36. Han S, Li H, Chen W, Yang L, Tong X, Zuo J, et al. Discovery of potent ebola entry inhibitors with (3*S*,4a*S*,8a*S*)2-(3-amino-2-hydroxypropyl) decahydroisoquinoline-3-carboxamide scaffold. *Eur J Med Chem* 2022;**240**:114608.
37. Xu D, Gong Y, Zhang L, Xiao F, Wang X, Qin J, et al. Modular biomimetic strategy enables discovery and SAR exploration of oxime macrocycles as influenza A virus (H1N1) inhibitors. *J Med Chem* 2024;**67**:8201−24.
38. Kim JI, Lee S, Lee GY, Park S, Bae JY, Heo J, et al. Novel small molecule targeting the hemagglutinin stalk of influenza viruses. *J Virol* 2019;**93**:e00878-19.
39. Prichard MN, Shipman Jr C. A three-dimensional model to analyze drug−drug interactions. *Antivir Res* 1990;**14**:181−205.
40. Van Dongen MJP, Kadam RU, Juraszek J, Lawson E, Brandenburg B, Schmitz F, et al. A small-molecule fusion inhibitor of influenza virus is orally active in mice. *Science* 2019;**363**:eaar6221.